The Critical Role of Aqueous-Phase Processes in Aromatic-Derived Nitrogen-Containing Organic Aerosol Formation in Cities with Different Energy Consumption Patterns

Yi-Jia Ma[1,2,3], Yu Xu[2,3]*, Ting Yang[1,2,3], Lin Gui[1,2,3], Hong-Wei Xiao[2,3], Hao Xiao[2,3], and Hua-Yun Xiao[2,3]

[1]School of Environmental Science and Engineering, Shanghai Jiao Tong University, Shanghai 200240, China

[2]School of Agriculture and Biology, Shanghai Jiao Tong University, Shanghai 200240, China

[3]Shanghai Yangtze River Delta Eco-Environmental Change and Management Observation and Research Station, Ministry of Science and Technology, National Forestry and Grassland Administration, Shanghai 200240, China

Yu Xu (E-mail: xuyu360@sjtu.edu.cn)

+8615885507087

Shanghai Jiao Tong University, 800 Dongchuan Road

Abstract. Nitrogen-containing organic compounds (NOCs) impact air quality and human health. Here, the abundance, potential precursors, and main formation mechanisms of NOCs in $PM_{2.5}$ during winter were compared for the first time among Haerbin (coal-dependent for heating), Beijing (natural gas and coal as heating energy), and Hangzhou (no centralized heating policy). The total signal intensity of CHON+, CHN+, and CHON− compounds was highest in Haerbin and lowest in Hangzhou. Anthropogenic aromatics accounted for 73%–93% of all identified precursors of CHON+, CHN+, and CHON− compounds in Haerbin. Although the abundance of aromatics-derived NOCs was lower in Beijing than in Haerbin, aromatics were also the main contributors to NOC formation in Beijing. Hangzhou exhibited the lowest levels of aromatic precursors. Furthermore, non-metric multidimensional scaling analysis indicated an overall reduction in the impact of fossil fuel combustion on NOC pollution along the route from Haerbin to Beijing to Hangzhou. We found that aqueous-phase processes (mainly condensation, hydrolysis or dehydration processes for reduced NOCs, and mainly oxidization or hydrolysis processes for oxidized NOCs) can promote the transformation of precursors to produce NOCs, leading to the most significant increase in aromatic NOC levels in Haerbin (particularly on haze days). Reduced precursor emissions in Beijing and Hangzhou (the lowest) constrained the aqueous-phase formation of NOCs. The overall results suggest that the aerosol NOC pollution in coal-dependent cities is mainly controlled by anthropogenic aromatics

40 and aqueous-phase processes. Thus, without effective emission controls, the

41 formation of NOCs through aqueous-phase processes may still pose a large threat to

42 air quality.

44 **Keywords:** Aerosols, Nitrogen-containing organic compounds, Energy structure,

45 Anthropogenic pollutants, Formation mechanisms

1. Introduction

Nitrogen-containing organic compounds (NOCs) are abundant reactive nitrogen species in aerosol particles, accounting for up to 40%–80% of total nitrogen deposition (Li et al., 2023; Xi et al., 2023; Yu et al., 2020). Clearly, aerosol NOCs can significantly contribute to the global nitrogen cycle (Li et al., 2023; Cape et al., 2011). Moreover, the formation of secondary organic aerosols (SOA) and light-absorbing organic aerosols (e.g., brown carbon) is also tightly associated with NOCs (Wang et al., 2024; Liu et al., 2023b; Zeng et al., 2021), thus affecting the radiative balance and air quality (Yuan et al., 2023; Jiang et al., 2023). In particular, certain NOCs, such as nitroaromatics and peroxyacyl nitrates, are characterized as phytotoxins and potential carcinogens, posing threats to ecosystems and human health (Shi et al., 2023; Singh and Kumar, 2022; Huang et al., 2024). Therefore, understanding the characteristics, origins, and atmospheric processes of NOCs is essential for comprehending their climate and health effects.

Aerosol NOCs can be derived from primary emissions associated with anthropogenic activities and natural sources (Lin et al., 2023; Xu et al., 2020a; Wang et al., 2017; Song et al., 2018; Song et al., 2022; Ma et al., 2024; Gui et al., 2024; Xu et al., 2024a). Secondary formation processes may play a more crucial role in the formation of NOCs in fine aerosol particles, which involve interactions among volatile organic compounds (VOCs), atmospheric oxidants, and reactive inorganic

67   nitrogen species (Montoya-Aguilera et al., 2018; Perraud et al., 2012; Hallquist et al.,

68   2009). For instance, laboratory studies have observed the formation of organic nitrates

69   from the oxidation of isoprene and α-/β-pinene by atmospheric oxidants and nitrogen

70   oxides (NO_x) (Surratt et al., 2010; Rollins et al., 2012; Nguyen et al., 2015).

71   Additionally, aqueous-phase reactions of NH_4^+ (or NH_3) with biogenic VOCs or

72   carbonyl compounds have been suggested to be important mechanisms of reduced

73   NOC (Re-NOCs) formation (Abudumutailifu et al., 2024; Laskin et al., 2014; Li et al.,

74   2019b; Liu et al., 2023b; Wang et al., 2024). However, understanding the origins,

75   formation mechanisms, and environmental impacts of NOCs is hindered by the

76   elusive and intractable molecular information regarding NOCs and their precursors.

77   Aerosol liquid water (ALW) can greatly increase the formation of aerosol NOCs

78   by facilitating the conversion of water-soluble organic gases into particles and

79   subsequently enabling aqueous-phase reactions (Li et al., 2019a; Lv et al., 2022; Liu

80   et al., 2023b). Several observational studies have found a positive correlation between

81   aerosol NOC abundance and either ALW or relative humidity (RH) (Jiang et al., 2023;

82   Liu et al., 2023b; Xu et al., 2020b). In particular, it has been suggested that increased

83   ALW levels can exacerbate winter haze in China (Wu et al., 2018; Hodas et al., 2014;

84   Lv et al., 2022; Wang et al., 2021d; Liu et al., 2023b; Wang et al., 2021a; Li et al.,

85   2019a). Presumably, precursors and ALW are the two key factors in the formation of

86   aerosol NOCs. Haze environments have potentially high RH levels and large

87   emissions of NOC precursors (Zheng et al., 2023; Nie et al., 2022; Liu et al., 2021;

88   Wang et al., 2021a). Moreover, in Chinese cities with different energy consumption

89   (e.g., coal, biomass, and natural gas) for winter heating (Zhang et al., 2021b; Zhang et

90   al., 2023b; Yang et al., 2024c), the types and emission intensities of pollutants

91   released from different heating sources are expected to vary considerably (Bond et al.,

92   2006; Stockwell et al., 2015; Křůmal et al., 2019). However, the potential effects of

93   ALW in the formation of NOCs in Chinese cities with different energy consumption

94   during winter, particularly in haze periods, are not well documented. Moreover, the

95   roles of ALW-related NOC formation processes in the formation of haze in cities with

96   different energy consumption types also remain largely unknown.

97   In this study, we present the measurements of the NOCs and other chemical

98   compositions in $PM_{2.5}$ collected from three cities (Haerbin, Beijing, and Hangzhou)

99   with different energy consumption during winter. The specific objectives of this study

100   were: (1) to investigate the differences in the abundance, composition, and major

101   precursors of NOCs in different cities with different energy consumption, especially

102   on polluted days; and (2) to elucidate the potential effects of aqueous-phase processes

103   on the formation of oxidized NOCs (Ox-NOCs) and reduced NOCs (Re-NOCs)

104   during winter (particularly on polluted days) in cities with different energy

105   consumption. The research findings are expected to provide valuable implications for

106   the mitigation of aerosol NOCs pollution in urban environments.

107

2. Materials and methods

2.1. Study site description and sample collection

The study sites are located in three urban areas, including Haerbin (HEB, i.e., Harbin, 126.64°E, 45.77°N), Beijing (BJ, 116.41°E, 40.04°N), and Hangzhou (HZ, 120.16°E, 30.30°N) (**Fig. S1**). The city of HEB, with a population of 9.95 million, is situated in the northeastern region of China. It relies heavily on coal for centralized heating during winter. The rapid urbanization and increased coal consumption have significantly deteriorated air quality in HEB in recent years (Ma et al., 2020). In contrast, BJ has largely shifted towards the utilization of cleaner energy sources (e.g., natural gas) for centralized heating in recent years, particularly following the implementation of the "Beijing 2013–2017 Clean Air Action Plan" (Vu et al., 2019; Yuan et al., 2023). HZ, situated within the Yangtze River Delta, is exempt from the necessity of heating due to the relatively mild winter climate (average temperature of 6.6 ± 2.4 °C during the sampling period, **Table S1**). Clearly, the distinctive energy consumption patterns observed in these three cities during winter provide a valuable opportunity to examine the impact of various precursors and aqueous-phase processes on aerosol NOC formation.

Sample collection was carried out simultaneously in three cities from 16 December 2017 to 14 January 2018. $PM_{2.5}$ samples were collected every two or three

127   days with a duration of 24 hours onto prebaked quartz fiber filters (Pallflex, Pall

128   Corporation, USA) using a high-volume air sampler (Series 2031, Laoying, China).

129   One blank sample was collected at each sampling site. A total of 39 samples were

130   collected, all of which were stored at −30°C. Meteorological data (e.g., temperature,

131   relative humidity (RH) and wind speed) together with concentrations of various

132   pollutants (e.g., SO_2 and NO_2) were obtained from nearby environmental stations. In

133   China, according to the Air Quality Index (MEEPRC, 2012), a pollution day is

134   defined as a day with a 24-hour average $PM_{2.5}$ concentration above 75 µg m^{-3}. This

135   standard has also been used in other studies performed in China (Zhang and Cao,

136   2015; Xu et al., 2024b; Yan et al., 2024), showing that the sampling periods were

137   classified as either "clean" or "haze" based on whether the daily average concentration

138   of $PM_{2.5}$ was below or above 75 µg m^{-3}.

139

140   **2.2. Chemical analysis**

141   The extraction and analysis methods for NOCs were consistent with those

142   described in our recent publication (Ma et al., 2024). Briefly, a portion of each filter

143   was extracted with methanol (LC-MS grade, CNW Technologies Ltd.) using

144   sonication in an ice bath (~4°C). The extracts were filtered through a 0.22 µm

145   polytetrafluoroethylene syringe filter and then concentrated to 300 µL under a gentle

146   stream of nitrogen gas. The concentrated extracts underwent composition analysis via

an ultra-performance liquid chromatography coupled with quadrupole time-of-flight

mass spectrometry equipped with an electrospray ionization (ESI) source (UPLC-ESI-

QToFMS, Waters Acquity Xevo G2-XS) (Wang et al., 2021c; Ma et al., 2024). This

analysis was done in both ESI+ and ESI– modes. The organic compounds were

separated on an Acquity HSS T3 column (2.1×100 mm, 1.8 µm particle size, Waters)

with an 18-minute gradient elution. The mobile phases comprised ultrapure water

with 0.1% formic acid (A) and methanol with 0.1% formic acid (B). Gradient elution

was conducted according to the following protocol: 1% B was held for 1.5 minutes,

followed by an increase to 54% B over a period of 6.5 minutes. Thereafter, the B was

increased to 95% over a period of 3 minutes. After reaching 100% B in one minute,

this state was maintained for 3 minutes. Finally, the concentration was returned to 1%

B in 0.5 minutes and held for 2.5 minutes. More detailed information about the

UPLC-ESI-QToFMS analysis can be found in **Sect. S1**. Due to uncertainties in

ionization efficiencies for different compounds (Ditto et al., 2022; Yang et al., 2023),

an intercomparison (mainly compared among samples within this study) of compound

relative abundance was conducted without accounting for differences in ionization

efficiency in the present study. This consideration was consistent with previous

studies (Xu et al., 2023; Jiang et al., 2022; Ma et al., 2024).

Another filter portion was ultrasonically extracted using Milli-Q water (~4°C ice

bath) to analyze the concentrations of inorganic ions and organic acids. The inorganic

167 ions (e.g., NO_3^-, SO_4^{2-}, Cl^-, Ca^{2+}, Mg^{2+}, Na^+, and NH_4^+) and organic acids (e.g.,

168 formic acid, acetic acid, oxalic acid, succinic acid, glutaric acid, and methanesulfonic

169 acid) were quantified using an ion chromatograph system (Dionex Aquion, Thermo

170 Scientific, USA), as described previously (Xu et al., 2022b; Yang et al., 2024b).

171

172 **2.3. Compound categorization and precursor identification**

173   The identified molecular formulas via UPLC-ESI-QToFMS were categorized

174 into different compound classes based on their elemental compositions, which

175 included CHO−, CHON−, CHONS−, and CHOS− in ESI− mode and CHO+, CHON+,

176 and CHN+ in ESI+ mode (Ma et al., 2024). Unless otherwise indicated, the molecular

177 formulas presented in the manuscript refer to neutral molecules. The "−" and "+"

178 symbols denote the detection ion modes, which correspond to ESI− and ESI+ modes,

179 respectively. Here, we mainly focus on NOCs (i.e., CHN+, CHON+, and CHON−

180 compounds) (Ma et al., 2024; Jiang et al., 2022; Wang et al., 2017). The carbon

181 oxidation state (OS_C) and double bond equivalent (DBE) were calculated to indicate

182 the oxidation level and unsaturation degree of the organics, respectively (**Sect. S2**)

183 (Kroll et al., 2011; Ma et al., 2024). Additionally, the modified aromaticity index

184 (AI_{mod}) and aromaticity equivalent (X_C) were used to evaluate aromaticity of organics

185 (Koch and Dittmar, 2006), as detailed in **Sect. S2**.

186   The potential precursors of NOCs were identified based on the methodology

187   described in previous studies (Nie et al., 2022; Guo et al., 2022; Jiang et al., 2023).

188   The classification of CHON+ and CHON− compounds was refined into following

189   categories, including aliphatics-, heterocyclics-, and aromatics-derived Re-NOCs

190   and isoprene-, monoterpenes-, aliphatics-, and aromatics-derived Ox-NOCs.

191   Moreover, CHN+ compounds were classified into aliphatic, monoaromatic, and

192   polyaromatic CHN+ compound (Wang et al., 2021b; Yassine et al., 2014). A detailed

193   description of the revised workflow for classifying NOCs according to potential

194   precursors was provided in **Sect. S3** and **Fig. S2**.

195

196   **2.4. Classification of potential pathways for NOC formation**

197   To identify potential aqueous-phase processes for aerosol NOC formation, we

198   screened precursor-product pairs from the organic compounds that have been detected

199   (Su et al., 2021; Xu et al., 2023; Jiang et al., 2023). The reaction pathways of Re-

200   NOCs (mainly CHON+ compounds in this study) were refined into the following

201   categories, including condensation (cond_N), hydrolysis (hy_N), dehydration (de_N),

202   cond_hy_N (involving cond_N and hy_N), cond_de_N (involving cond_N and de_N),

203   hy_de_N (involving hy_N and de_N), cond_hy_de_N (involving cond_N, hy_N and

204   de_N) and unknown_N (unknown processes) formation pathways (**Fig. S3 and Table**

205   **S4**) (Sun et al., 2024; Abudumutailifu et al., 2024; Laskin et al., 2014; Liu et al.,

206   2023c). Another significant class of Re-NOCs is the CHN+ compounds. Their

207   potential formation mechanisms include cond_N, de_N, cond_de_N, and other

208   unidentified (unknown_N) pathways (**Fig. S4** and **Table S4**) (Abudumutailifu et al.,

209   2024; Laskin et al., 2014; Liu et al., 2023c). In addition, the reaction pathways of Ox-

210   NOCs (mainly CHON− compounds in this study) were refined into the following

211   categories, including ox_N, hy_N, ox_hy_N (involving ox_N and hy_N), and other

212   unidentified (unknown_N) pathways (Jiang et al., 2023; Su et al., 2021) (**Fig. S5** and

213   **Table S4**). A detailed overview of the methodologies employed to discern potential

214   NOC formation pathways was shown in **Sect. S4**, **Table S4,** and **Figs. S3–S5**.

215   It is important to acknowledge the potential limitations in the categorization

216   methodology of NOC formation pathways described above. This is because the

217   approach applied here and in previous studies (Jiang et al., 2023; Su et al., 2021) may

218   classify NOCs as products of aqueous-phase reactions from primary emissions.

219   Accordingly, our results can be regarded as a maximal potential (or an upper limit) for

220   NOC generation from aqueous-phase reactions. In particular, certain reaction

221   pathways (e.g., oligomerization) were not included in this study due to the complexity

222   of the atomic changes involved, which could not be effectively characterized using the

223   "precursor-product pairs" approach. In this study, NOCs produced from the reaction

224   pathways identified by the abovementioned classification methodology can explain 76%

225   of CHON+ compounds, 61% of CHN+ compounds, and 65% of CHON− compounds.

226   Thus, the classification of potential pathways for NOC formation was representative,

227   at least in this study.

228

229   **2.5. More parameter calculations and data analysis**

230   A thermodynamic model (ISORROPIA-II) was used to estimate the ALW

231   concentration and pH value, as described in previous studies (Xu et al., 2020b; Xu et

232   al., 2023; Xu et al., 2022c). Ambient hydroxyl radical (•OH) concentrations were

233   predicted using empirical formulas proposed by Ehhalt and Rohrer (2000), which was

234   reported in detail in our previous field observations (Liu et al., 2023a; Lin et al., 2023).

235   The ventilation coefficient (VC) is an indicator of the potential for atmospheric

236   dilution of pollutants, which was calculated by multiplying the wind speed by the

237   planetary boundary layer height (PBLH) (Gani et al., 2019) .

238   Non-metric multidimensional scaling (NMDS) was employed to visualize the

239   distributions of NOCs (CHON+, CHN+, and CHON− compounds) in two dimensions,

240   based on Bray-Curtis distances (Chao et al., 2006). The stress values ranged from

241   0.03 to 0.11 (less than 0.2, **Table S5**) in our analysis, indicating that the differences

242   among samples can be well represented in the two-dimensional pattern. To further

243   assess the influence of anthropogenic emissions and aqueous-phase processes on the

244   distribution of NOCs, the envfit function in the R package Vegan (Oksanen et al.,

245   2007) was utilized. Furthermore, the Spearman rank correlation, a non-parametric

246   measure with less sensitivity to outliers and independent of data distribution

247   assumptions, was employed to examine the association patterns between NOCs and

248   the parameters related to anthropogenic emissions and aqueous-phase processes

249   (Kellerman et al., 2014).

250

251   **3. Results and discussion**

252   **3.1. Overview of pollution and aerosol NOC characteristics in different cities**

253   **Figure 1a–c** and **Table S1** show the variations in major gaseous pollutants, $PM_{2.5}$

254   and its major compositions, as well as meteorological parameters in three Chinese

255   cities with different energy consumptions during winter. The average $PM_{2.5}$

256   concentration in HEB was 90.6 ± 62.4 μg m^{-3}, which was significantly higher than

257   that observed in BJ (52.7 ± 51.4 μg m^{-3}) and HZ (69.1 ± 29.6 μg m^{-3}). Similarly, the

258   concentrations of SO_2 and nss-Cl$^-$ were higher in HEB than in BJ and HZ. In addition,

259   a lower NO_3^-/SO_4^{2-} mass ratio (**Table S1**) was found in HEB. SO_2 and nss-Cl$^-$ have

260   been suggested to be typical pollutants emitted from coal combustion during winter in

261   cities (Zhao and Sun, 1986; Streets and Waldhoff, 2000). The low NO_3^-/SO_4^{2-} mass

262   ratio can indicate a predominance of stationary sources (e.g., coal combustion) (Wang

263   et al., 2006; Arimoto et al., 1996; Xiao and Liu, 2004). These results suggest that coal

264   combustion during the winter heating season in HEB may significantly contributed to

265   severe $PM_{2.5}$ pollution. This consideration can also be supported by the highest coal

266   consumption in HEB in 2017–2018 (**Fig. 1d**). Due to the large-scale use of clean

267   energy (i.e., natural gas) in BJ (**Fig. 1e**), the coal consumption in BJ was the lowest

268   (**Fig. 1d**). This resulted in the lowest pollutant levels in BJ. From clean to polluted

269   days, HEB and BJ showed larger increases in pollutant levels (e.g., $PM_{2.5}$, SO_2, and

270   CO), followed by HZ. Thus, the release of pollutants caused by the use of fossil fuels

271   for centralized heating in winter (only occurred in HEB and BJ) was undoubtedly one

272   of the important factors contributing to the generation of haze in HEB and BJ.
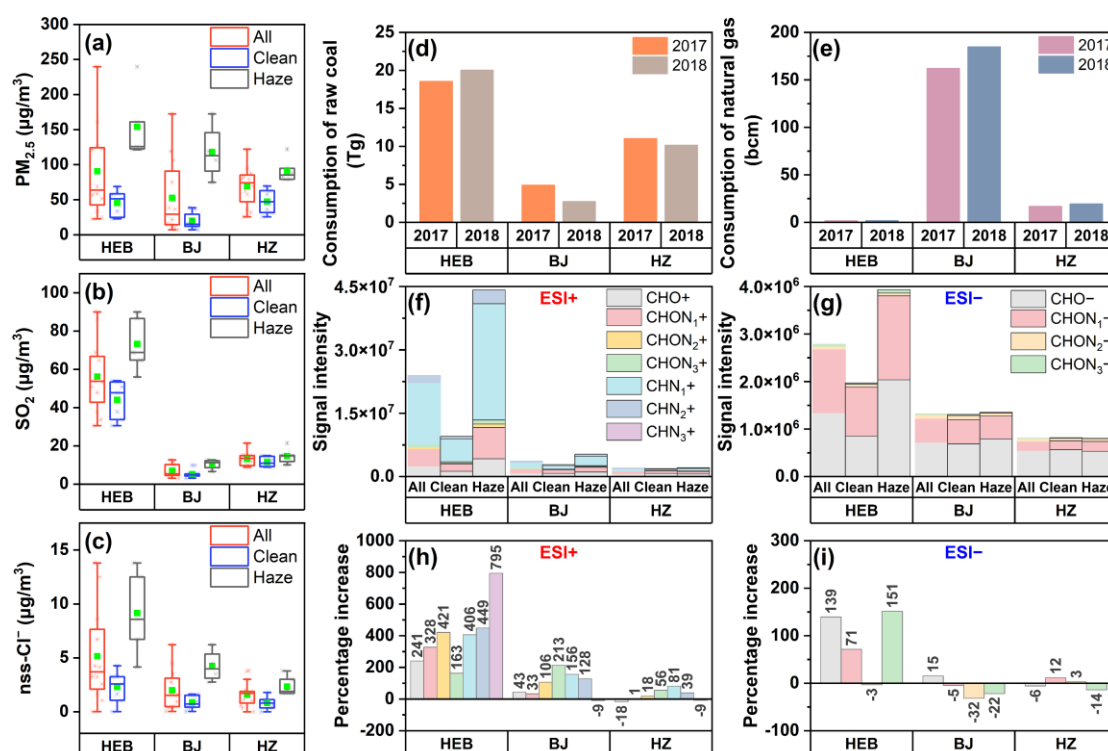
273

274   **Figure 1.** Box and whisker plots showing variations in the concentration of (**a**) $PM_{2.5}$,

275   (**b**) SO_2, and (**c**) nss-Cl^- in all (gray), clean (blue), and haze (red) periods in different

276   cities. Each box encompasses the 25th–75th percentiles. Whiskers are the 5th and

277   95th percentiles. The green squares and solid lines inside boxes indicate the mean and

278   median value. The consumption of (**d**) raw coal and (**e**) natural gas in 2017 and 2018

279   in different cities was obtained from the local statistical yearbooks. Average

280   distributions in the signal intensity of species detected in $PM_{2.5}$ collected during

281   different winter periods in different cities in (**f**) ESI+ and (**g**) ESI− modes. Percentage

282   variations in the signal intensity of each subgroup from clean to haze periods in

283   different cities in (**h**) ESI+ and (**i**) ESI− modes.

284

285   **Figure 1f** and **g** show the average signal intensity distributions of organic

286   compounds detected in $PM_{2.5}$ across sampling periods in different cities. The detailed

287   mass spectra of organic compounds detected in ESI+ and ESI− were shown in **Fig. S6**.

288   CHN_1+ ($n = 437−448$) compounds were the main CHN molecules measured in ESI+

289   mode in all cities (**Fig. 1f** and **Table S6**), the signal intensity of which accounted for

290   over 77% of the total $CHN_{1−3}+$ signal intensity. Similarly, $CHON_1+$ compounds ($n =$

291      $398−421$) dominated in $CHON_{1−3}+$ molecules, with a higher signal intensity than

292      $CHON_{2−3}+$ (**Fig. 1f** and **Table S6**). The high abundances of CHN_1+ and $CHON_1+$

293   compounds in NOCs were similar to previous reports about the NOC characteristics

294   of urban aerosols (He et al., 2024; Abudumutailifu et al., 2024). The signal intensity

295   fractions (40%−77%) of CHN+ compounds in total NOCs in these three cities were

296   higher than those observed (8.20%−17.47%) during winter in Ürümqi where the same

297   NOC analysis method was conducted (Ma et al., 2024). However, the signal intensity

298   fractions of CHON+ compounds in total NOCs were lower in these three cities

299 (23%−60%) than in Ürümqi (over 82.53%) (Ma et al., 2024). More frequent biomass

300 burning and relatively dry climate in Ürümqi (northwest China) (Ma et al., 2024) may

301 result in different sources and formation processes of NOCs compared to this study.

302 The signal intensity of these NOCs detected in ESI+ mode varied across cities, with

303 the highest CHN+ and CHON+ signal intensities in HEB, followed by BJ and HZ.

304 Moreover, we found that the total signal intensities of CHN+ and CHON+ compounds

305 increased by 382% in HEB from clean to haze periods, followed by increase of 102%

306 in BJ and increase of 31% in HZ (**Fig. 1h** and **Table S6**). This variation pattern of

307 CHN+ and CHON+ compounds from clean to haze periods was similar to that of the

308 pollutants mentioned previously (**Fig. 1a–c**). Given the high sensitivity of ESI+ mode

309 to protonatable species, reduced species (e.g., amine- and amide-like compounds)

310 were expected to predominate the NOCs (Han et al., 2023; Wang et al., 2018), the

311 formation of which was highly related to precursor emission level, aerosol acidity, and

312 ALW concentrations (Kuwata and Martin, 2012; Vione et al., 2005; Yang et al., 2024a;

313 Xu et al., 2020b). Thus, these results suggest that there may be significant differences

314 in the sources, precursor emission intensity, or main formation pathways of NOCs in

315 different energy consuming cities.

316   The number of NOCs identified in ESI− (296–301 molecules excluding sulfur-

317 containing compounds, **Table S7**) was found to be lower than that observed in ESI+

318 (1346–1361) (**Table S6**). This finding was similar to previous observations about the

319   NOCs of urban organic aerosols in Beijing, Mainz, Changchun, Guangzhou, and

320   Shanghai (Wang et al., 2021b; Wen et al., 2023; Wang et al., 2018). $CHON_1-$

321   compounds were the main NOC molecules in ESI− mode in all cities (**Fig. 1g** and

322   **Table S7**). The average signal intensity of CHON− compounds was highest in HEB,

323   followed by BJ and HZ. Moreover, the outbreak of $CHON_{1-3}$ signal intensity during

324   polluted periods was found in HEB, whereas insignificant increases occurred in BJ

325   and HZ (**Fig. 1i**). Deprotonated NOCs with oxidized nitrogen-functional groups, such

326   as nitro ($-NO_2$) or nitrooxy ($-ONO_2$) groups, are more sensitive to the ESI− mode

327   (Wang et al., 2017; Jiang et al., 2023; Yuan et al., 2023). Clearly, the formation of

328   aerosol CHON− compounds was largely dependent on atmospheric oxidation capacity

329   and gas- and aqueous-phase reactions (Ng et al., 2017; Shi et al., 2020; Shi et al.,

330   2023). Thus, the differences in CHON− compound abundance in different polluted

331   periods and cities together with the spatiotemporal changes in CHN+ and CHON+

332   abundances mentioned previously were likely attributed to variations in sources,

333   mechanisms, or key influencing factors of NOC formation in these three cities, which

334   will be further discussed in the following sections.

335

336   **3.2. Potential precursors of aerosol NOCs in different cities**

337   **Figure 2** presents the average signal intensity percentage and signal intensity

338   distributions of different NOCs from various precursors in different cities during

339   winter. Aromatics-, heterocyclics-, and aliphatics-derived Re-NOCs together

340   accounted for more than 74% (74%–79%) of the total signal intensity of CHON+

341   compounds in the three study cities (**Fig. 2a–c** and **Table S8**). Specifically, the

342   proportion of the aromatics-derived CHON+ signal intensity in the total CHON+

343   signal intensity was much higher in HEB (73%) than in BJ (33%), with the lowest

344   proportion observed in HZ (23%) (**Fig. 2a–c**). Furthermore, we observed that

345   aromatic CHN+ compounds (mono- and poly-aromatics) dominated the total CHN+

346   compounds in both number and abundance in all investigated cities (**Table S9** and **Fig.**

347   **2d–f**). The average signal intensity percentage and signal intensity of aromatic CHN+

348   compounds were also highest in HEB (**Fig. 2d–f** and **k**). The calculated AI_{mod} values

349   for CHON+ and CHN+ compounds were higher in HEB than in BJ and HZ (**Table**

350   **S10**), which further indicated a higher aromaticity of these NOCs in HEB. It has been

351   suggested that coal combustion can release a large amount of aromatic compounds

352   (Zhang et al., 2023a), which potentially increased NOC aromaticity (Yuan et al.,

353   2023). Thus, the higher signal proportion of aromatics-derived Re-NOCs in HEB can

354   be explained by the higher coal combustion emissions during winter. In contrast, the

355   use of clean energy during the central heating season in BJ and the reduced emissions

356   in HZ without central heating weakened the formation of aerosol aromatic NOCs.

357   CHON− compounds were also primarily dominated by aromatics-derived Ox-

358   NOCs in all three cities, accounting for more than 73% (73%–90%) of the total signal

359   intensity of CHON− compounds, on average (**Fig. 2g–i**). This finding was consistent

360   with field observations conducted in other Chinese cities such as Shanghai,

361   Changchun, Guangzhou, and Wangdu during winter (Wang et al., 2021b; Jiang et al.,

362   2023). The abundance of aromatics-derived Ox-CHON− compounds and the AI_{mod}

363   value of CHON− were highest in HEB and decreased sequentially in BJ and HZ (**Fig.**

364   **2l** and **Table S10**), further indicating our previous consideration that coal combustion

365   heating in HEB can lead to higher NOC pollution. It is worth noting that the

366   percentage of total signal intensity of Ox-NOCs with biogenic VOCs (BVOCs) as

367   precursors was less than 3% (**Fig. 2g–i** and **Table S8**). This can be partly supported by

368   the previous observations showing that anthropogenic VOCs (AVOCs) were the main

369   contributors to the formation of Ox-NOCs (e.g., organic nitrates) in urban areas in

370   China (Wang et al., 2021b; Jiang et al., 2023). The overall results suggest the

371   significant role of AVOCs in the formation of NOCs in all investigated cites,

372   particularly in HEB.

373
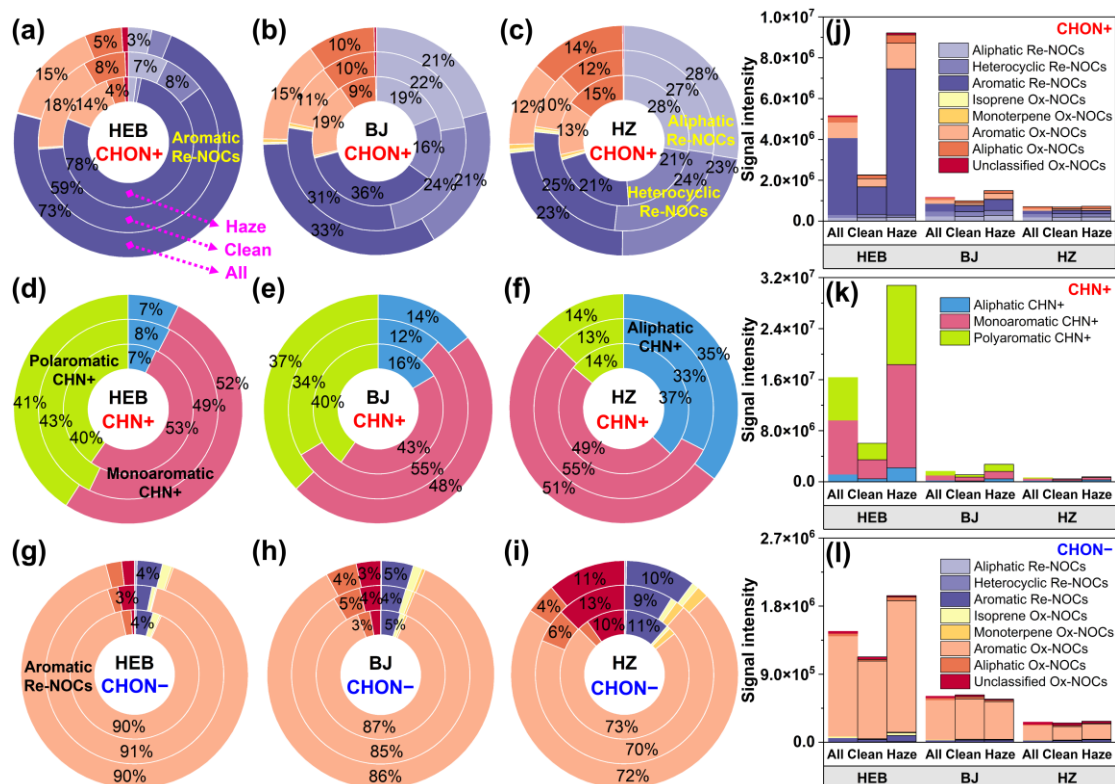
Figure 2. Average percentage distributions of signal intensities for (**a**–**c**) CHON+, (**d**–**f**) CHN+, and (**g**–**i**) CHON− compounds from various sources in PM$_{2.5}$ collected from different cities during winter. Average signal intensity distributions for (**j**) CHON+, (**k**) CHN+, and (**l**) CHON− compounds from various sources in PM$_{2.5}$ collected from different cities during winter.

From clean to haze periods, the signal intensities of all aromatics-derived CHON compounds increased significantly in HEB (**Figs. 2a, j, g, l** and **S7**). In contrast, the signal intensities of aromatics-derived CHON compounds in BJ and HZ showed an insignificant increase during haze periods. In addition, the average values of O/C$_w$ and OS$_{Cw}$ for CHON+ and CHON− compounds were higher in HEB than in BJ (second

385 highest) and HZ, and their increases from clean to haze periods were also greater in

386 HEB (**Table S10**). Concurrently, the O/C_w ratio of aerosol NOCs in HEB was

387 observed to be higher than that of coal-derived aerosols (Song et al., 2018). Heald et

388 al. (2010) previously demonstrated that oxidation processes can lead to an increase in

389 the O:C ratio of organic aerosols. These results indicated that aerosol NOCs in HEB

390 were more oxidized aromatics (or aged aromatics), particularly during haze. The

391 average N/C_w ratios of CHON+ and CHON− compounds in HEB (0.13 and 0.15,

392 respectively) (**Table S10**) were higher than those of CHON+ (0.079) and CHON−

393 (0.07) compounds in aerosols directly emitted from coal combustion (Song et al.,

394 2022; Song et al., 2018). The N/C_w ratios were also higher in HEB than in BJ and HZ

395 and increased during hazy days (0.13 for CHON+ and 0.16 for CHON− in hazy days

396 in HEB). It has been suggested that the N/C_w ratio of CHON− compounds tended to

397 increase (from 0.109 to 0.119) after aging of fuel combustion-derived aerosols (Zhao

398 et al., 2022a). Thus, these results, combined with previous analysis of potential

399 precursors for NOCs, suggest that anthropogenic precursor emissions and their

400 atmospheric transformation to form CHON compounds were stronger in HEB than in

401 BJ and HZ. Moreover, considering that the emission intensity of precursors during

402 clean and hazy days may not significantly change, secondary processes may

403 significantly promote the formation of NOCs in HEB during hazy days (the most

404 significant increase in NOC abundance). However, this promoting effect during hazy

405   days was insignificant in BJ and HZ (less increase in NOC abundance).

406

407   **3.3. Main factors influencing aerosol NOC formation in different cities**

408   As discussed in the previous section, the results indicated that AVOCs play a

409   significant role in the formation of NOCs. Furthermore, secondary processes may

410   contribute to NOC formation to varying extents in different cities. This section

411   provides a detailed discussion of the key factors influencing the molecular distribution

412   of NOCs. First, a Spearman correlation analysis was performed to examine the

413   relationship between various parameters and NOCs (**Fig. 3** and **Figs. S8−S12**). The

414   peak intensity of most CHON+ compounds (mainly aromatics, as mentioned

415   previously) showed a strong correlation ($P < 0.01$) with the concentrations of

416   combustion source-related tracers (e.g., SO_2, nss-Cl^-, nss-K^+, CO, and NO_2) (Zhao

417   and Sun, 1986; Streets and Waldhoff, 2000; Shen et al., 2009; Zhang et al., 2011;

418   Mafusire et al., 2016; Liu et al., 2019; Zhang et al., 2021a; Wang et al., 2020) in HEB

419   (**Figs. 3a** and **S8a–d**). Although there was a significant correlation ($P < 0.05$) between

420   most CHON+ compounds and those combustion source indicators in BJ, the strength

421   of this correlation was weaker in BJ than in HEB (**Figs. 3e** and **S8f–i**). However,

422   similar significant correlations between them were not observed in HZ (**Figs. 3i** and

423   **S8k–n**). Thus, the greatest contribution of anthropogenic activities to the formation of

424   CHON+ compounds in winter was in HEB (central heating with coal), followed by BJ

425   (central heating with coal and natural gas) and HZ (without central heating). Most of

426   CHN+ and CHON− compounds showed a similar spatial response pattern to those

427   anthropogenic activities (**Figs. S9** and **S10**). These results are consistent with the

428   previous analysis of NOC precursors (**Fig. 2**), which concluded that the intensity of

429   anthropogenic pollutant emissions in different energy consuming cities was an

430   important factor affecting the formation of NOC and causing spatial differences in

431   NOC abundance.
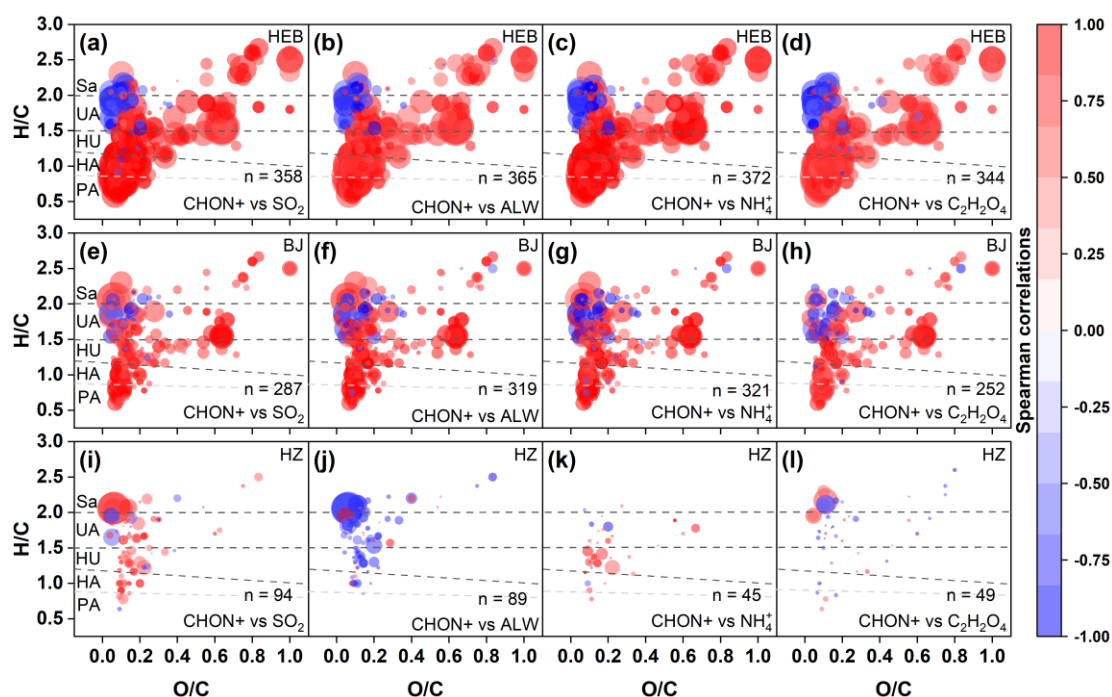
432

433   **Figure 3.** Spearman rank correlation coefficients (with $P < 0.01$ in HEB and $P < 0.05$

434   in BJ and HZ) of individual CHON+ molecules with selected parameters in (**a–d**)

435   HEB, (**e–h**) BJ and (**i–l**) HZ. The color scale indicates Spearman correlations between

436   the intensity of individual CHON+ molecules and each parameter. The symbol n in

437   the bottom right corner of each panel indicates the number of molecular formulas

438 significantly correlated with the variables. The subgroups in the panels include

439 polycyclic aromatic-like (PA), highly aromatic-like (HA), highly unsaturated-like

440 (HU), unsaturated aliphatic-like (UA), and saturated-like (Sa) compounds.

441

442 Furthermore, we found that the peak intensities of most CHON+, CHN+, and

443 CHON− compounds (mainly aromatics) were significantly correlated ($P < 0.01$) with

444 the concentrations of ALW, NH_4^+, oxalic acid, and SO_4^{2-} (**Figs. 3b–d**, **S8e**, and

445 **S11**–**S12**) in HEB. The correlations between these NOCs and parameters weakened in

446 BJ and disappeared in HZ (**Figs. 3**, **S8**, and **S11**–**12**). It is generally accepted that

447 SO_4^{2-}, NH_4^+, and NO_3^- in fine aerosols are primarily formed through secondary

448 processes (Gao et al., 2021; Wang et al., 2021d). NH_4^+ can serve as a key reactant in

449 the formation of aerosol NOCs (e.g., "carbonyl-to-imine" transformation) in the

450 aqueous-phase (Laskin et al., 2014; Lee et al., 2013; Li et al., 2019b). Oxalic acid

451 ($C_2H_2O_4$) has been identified as a marker (defined by Nozière et al. (2015)) for

452 aqueous-phase SOA (Xu et al., 2022a; Chen et al., 2021). Additionally, numerous

453 laboratory and field observational studies have shown that ALW can promote the

454 formation of NOCs (Lv et al., 2022; Liu et al., 2023b; Jimenez et al., 2022; Jiang et al.,

455 2023). Thus, these results indicate that aqueous-phase processes can significantly

456 promote the formation of NOCs in HEB, however, as the precursor emission intensity

457 gradually decreased in BJ and HZ, this aqueous-phase promoting effect also

458   decreased.

459   The NMDS analysis between various parameters and NOCs was conducted to

460   further investigate the variations in key factors affecting the formation of NOCs from

461   clean to haze days (**Fig. 4**). The formation of CHON+, CHN+, and CHON−

462   compounds with higher AI_{mod} values (mainly aromatics, as mentioned previously)

463   during haze days in HEB and BJ were closely associated with the factors indicating

464   anthropogenic precursor emissions and aqueous-phase reaction processes. In contrast,

465   the level of oxidants (i.e., O_3 and •OH) played a more important role during clean

466   days in HEB and BJ, driving more highly saturated NOC formation during clean days

467   (**Fig. 4**). A reasonable explanation for this is that the solar radiation and •OH levels on

468   polluted days were lower than those on clean days (**Table S1**). The impacts of various

469   factors on the formation of aerosol NOCs showed a weak discrimination between

470   haze and clean days in HZ (**Fig. 4c, f** and **i**). Laboratory studies have shown that

471   reactive components (e.g., •OH and H_2O_2) in the aqueous phase can continuously

472   convert low-solubility organics to form aqueous phase SOA (Chen et al., 2008; Huang

473   et al., 2011; Dong et al., 2021). Field observations also suggested that precursors

474   (most of them are aromatic compounds) released from the combustion of fossil fuels

475   significantly contributed to the aqueous SOA formation (> 50% total molecules) (Xu

476   et al., 2022a) through the rapid aqueous-phase conversion of primary organic aerosol

477   (POA) to SOA at high RH (Wang et al., 2021a). This implies that higher precursor

478   abundance can drive more aerosol NOC formation via aqueous-phase processes. As

479   mentioned previously, the emission intensity of precursors decreased sequentially

480   from HEB to BJ and then to HZ. Moreover, the ALW concentrations were much

481   higher on polluted days than on clean days in three investigated cities. The rising

482   ALW during the pollution period and the quiescent steady state of the atmosphere

483   favored the formation of SOA from anthropogenic emission precursors (Guo et al.,

484   2014; He et al., 2018). Thus, the above discussion can suggest that the spatial

485   differences in precursor emission intensity (higher in HEB) and enhancement of

486   aqueous-phase processes in polluted days were the main factors leading to the

487   differences in the proportion (higher in HEB) of increase in NOC abundance from

488   clean days to polluted days in three different energy consuming cities. In addition, the

489   increased VC value (**Table S1**) in clean days (beneficial for the diffusion of pollutants)

490   (Gani et al., 2019) was also an important factor limiting the abundance of NOCs (**Fig.**

491   **4**), resulting in a lower NOC abundance on clean days compared to polluted days (**Fig.**

492   **1**).
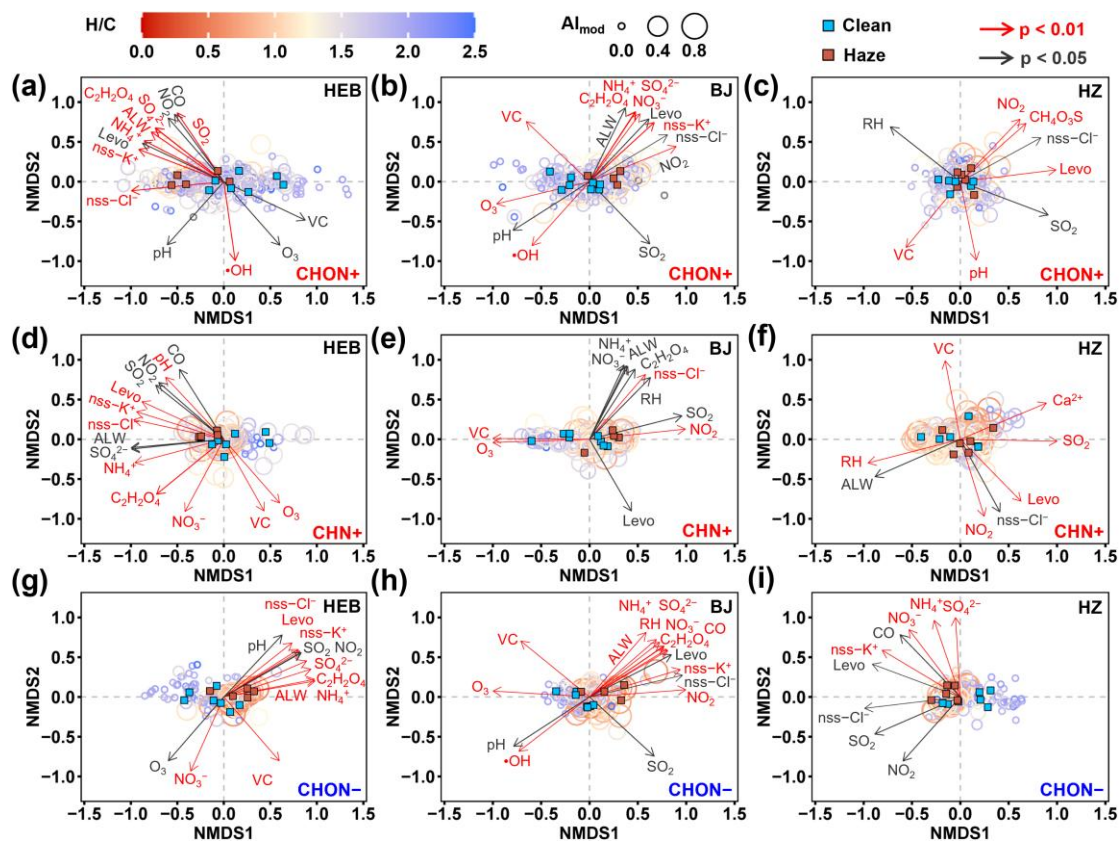
Figure 4. Nonmetric multidimensional scaling of (**a**–**c**) CHON+, (**d**–**f**) CHN+, and (**g**–**i**) CHON− compounds from organic aerosol in different cities. The color and size of the circle indicate the H/C ratio and AI$_{mod}$ value of compounds, respectively. Significant relationships between the variables and ordination (999 permutations) are indicated by $p < 0.05$ (grey) and $p < 0.01$ (red). Insignificant correlations are not shown. The scores of the samples collected during clean and haze periods were shown as blue and brown squares, respectively.

As mentioned above, the aerosol NOCs of HZ were less affected by anthropogenic pollutants emitted from coal and natural gas combustion compared to

504   HEB and BJ with centralized heating. Interestingly, we found that the molecular

505   distributions of most aromatic CHON+ compounds in HZ were not only influenced

506   by some anthropogenic pollutants (e.g., SO_2 and NO_2), but also by methanesulfonic

507   acid (CH_4O_3S) (**Fig. 4c**). Moreover, neither CHN+ nor CHON+ exhibited significant

508   correlations with factors related to secondary processes in HZ (**Fig. 4c** and **f**).

509   Methanesulfonic acid has been suggested to be a tracer for ocean aerosols (Ayers and

510   Gras, 1991; Suess et al., 2019). These results suggest that aerosol CHON+

511   compounds in HZ may be influenced by long-distance transport air masses originating

512   from the ocean. This consideration can be also supported by the fact that only HZ was

513   affected by air masses originated from the ocean (**Fig. S13**). Thus, marine emissions

514   may be an important contributor to aerosol NOCs in HZ, which was significantly

515   different from the cases of HEB and BJ where aromatic pollutants from fossil fuel

516   combustion and aqueous-phase processes control the composition and abundance of

517   aerosol NOCs.

518

519   **3.4. Potential formation mechanisms of aerosol NOCs in cities with different**

520   **energy consumption**

521   **Figure 5** shows the average signal intensity percentage and signal intensity

522   distributions of NOCs formed by different aqueous-phase processes (**Table S4** and

523   **Figs. S3–S5**) in different cities during winter. The identification of specific reaction

pathways was detailed in **Figs. S3–S5** and **Sect. S4**. During the entire study period,

the cond_N, cond_hy_N, and cond_de_N pathways together accounted for more than

68% (68%−74%) of the total signal intensity of CHON+ compounds in the three cities

(**Fig. 5a–c** and **Table S11**). Specifically, the formation of CHON+ compounds was

mainly dominated by the cond_N and cond_hy_N pathways in HEB, with less impact

from the cond_de_N pathway (**Fig. 5a**). However, CHON+ compounds derived from

the cond_de_N pathway showed a much higher proportion in BJ and HZ than in HEB

(**Fig. 5b** and **c**). The cond_de_N pathway involves both condensation and dehydration

processes (**Table S4 and Fig. S3**). Recent studies have identified that dehydration

reactions may occur in aerosols and fog water (Sun et al., 2024), as well as in

photochemical transformations of organic compounds in aqueous phase (Lian et al.,

2020). While the exact pathways of dehydration reactions in the particle phase remain

uncertain, stronger solar radiation in BJ and HZ than in HEB (**Table S1**) may partly

explain the higher signal proportion of CHON+ compounds formed through the

cond_hy_N pathway in BJ and HZ. Furthermore, the higher signal proportions of

CHN+ compounds formed through the de_N pathway in BJ (6%) and HZ (11%) than

in HEB (2%) may also be associated with this solar radiation-induced dehydration

mechanism (**Fig. 5d–f** and **Table S12**). For CHN+ compounds, the cond_de_N

process dominated their formation (**Fig. 5d–f**). In general, the cond_N, cond_hy_N,

and cond_de_N processes contributed most significantly to the formation of Re-NOCs

544   in HEB, followed BJ and HZ.
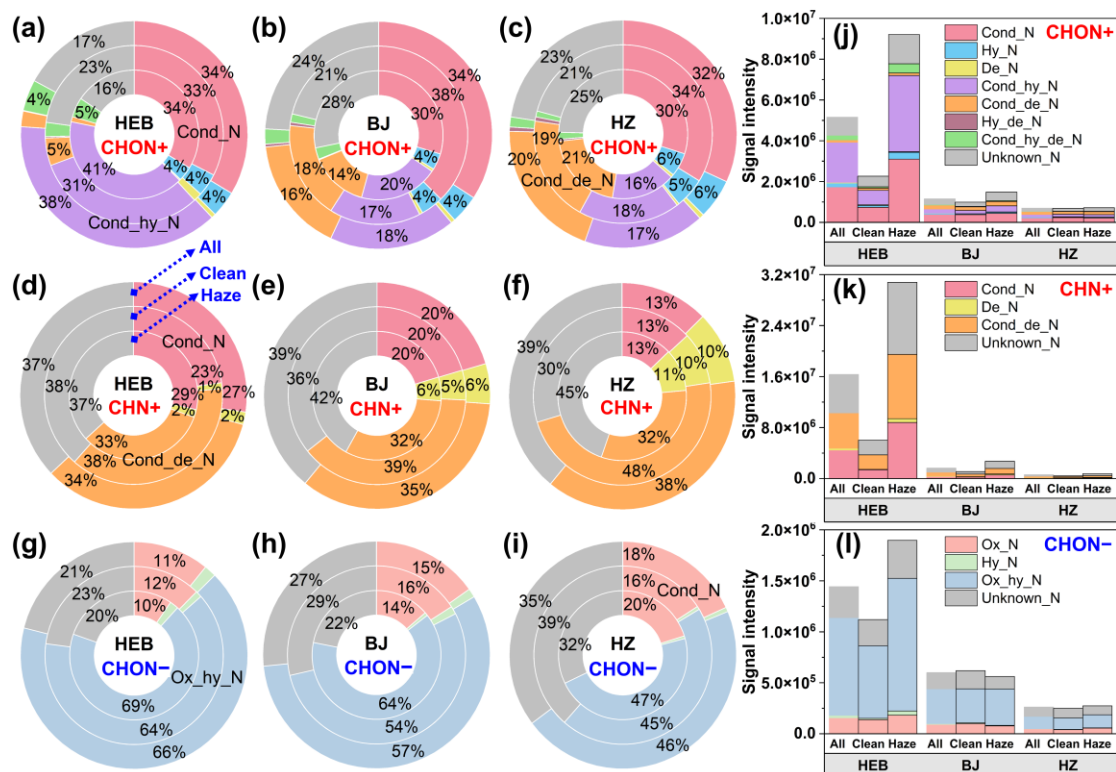
Figure 5. Average percentage distributions of signal intensities for aerosol (**a–c**) CHON+, (**d–f**) CHN+, and (**g–i**) CHON− compounds from various reaction pathways in different cities during winter. Average signal intensity distributions for aerosol (**j**) CHON+, (**k**) CHN+, and (**l**) CHON− compounds from various reaction pathways in different cities during winter.

552   A typical mechanism for Re-NOC formation is the aqueous-phase reactions

553   between carbonyl compounds and NH_4^+ (or NH_3) (Abudumutailifu et al., 2024;

554   Laskin et al., 2014; Li et al., 2019b; Liu et al., 2023b; Wang et al., 2024). If this

555   mechanism is simplified as a second-order reaction (i.e., [Precursor] + [NH_3 and NH_4^+]

556 ↔ [Re-NOCs]), the production of Re-NOCs is expected to be proportional to the

557 abundances of precursor and NH_4^+ (Yang et al., 2023; Lin et al., 2023). Indeed, the

558 signal intensities of the Re-CHON+ and Re-CHN+ compounds were significantly

559 positively correlated with the signal intensities of their CHO precursors (identified

560 using the precursor-product pairs theory, **Figs. S3** and **S4**) and NH_4^+ concentration in

561 HEB (**Fig. 6a, b, d** and **e**). This correlation gradually weakened from BJ to HZ (**Fig.**

562 **6a, b, d** and **e**). As previously discussed, differences in energy consumption patterns

563 resulted in the highest levels of anthropogenic aromatic compound emissions in HEB

564 during the winter, followed by BJ, with the lowest levels in HZ (**Figs. 2** and **S14**).

565 Thus, the signal intensities of CHON+ and CHN+ compounds from cond_N,

566 cond_de_N, and cond_hy_N processes were higher in HEB than in BJ and lowest in

567 HZ (**Fig. 5j** and **k**).
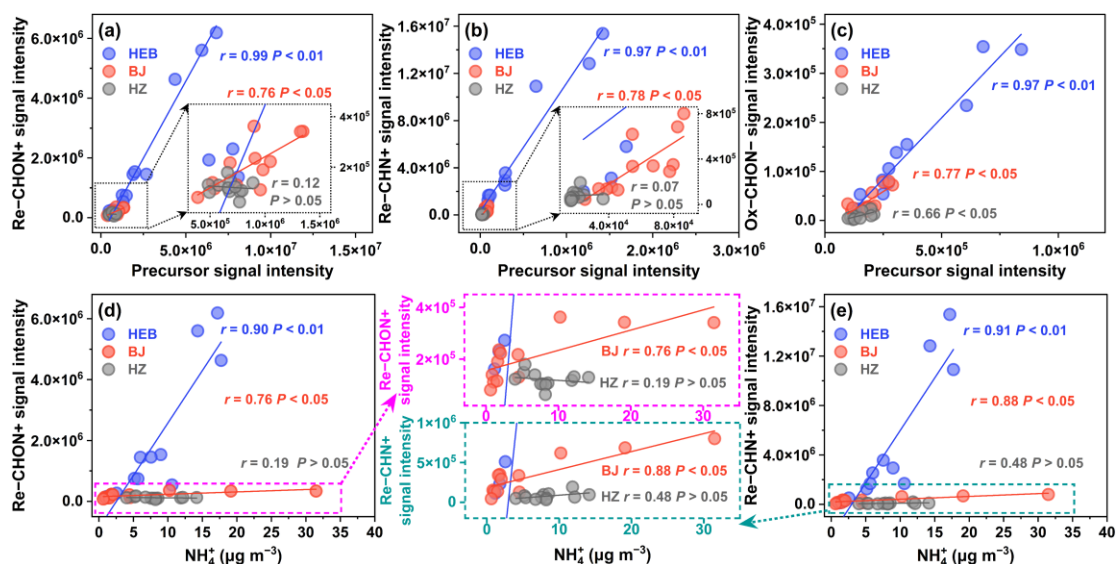
569 **Figure 6.** Signal intensity of (**a**) Re-CHON+, (**b**) Re-CHN+, and (**c**) Ox-CHON−

570 compounds as functions of signal intensity of precursors (CHO compounds). Signal

571   intensity of (**d**) Re-CHON+ and (**e**) Re-CHN+ compounds as functions of the

572   concentrations of NH_4^+.

573

574   Additionally, we noticed that the contribution of these aqueous-phase processes to

575   the formation of CHON+ and CHN+ compounds increased significantly from clean to

576   hazy days in HEB and BJ (**Fig. 5**). The increased ALW concentrations (**Table S1**) and

577   atmospheric stability during haze periods likely provided favorable conditions for the

578   precursors to undergo these aqueous-phase reactions, resulting in the formation of

579   NOCs. Clearly, high pollutant emission levels in HEB provided a greater potential to

580   convert precursors into more NOCs via the cond_N, cond_hy_N, and cond_de_N

581   processes during haze periods. Thus, the hazy days in the HEB showed the largest

582   increase in CHON+ and CHN+ compounds from the cond_N, cond_hy_N, and

583   cond_de_N processes (**Fig. 5j** and **k**). In contrast, due to generally mild winters

584   leading to the absence of heating and the implementation of stricter pollution control

585   measures (more coal usage in HZ than in BJ, as shown in **Fig. 1d**), the precursor

586   emissions in HZ were lower. These emissions were insufficient to support the

587   production of large amounts of NOCs in the aqueous phase. These results also

588   indicate that emission reduction is the key to controlling aerosol NOC pollution.

589   CHON− compounds derived from the ox_hy_N and ox_N processes together

590   accounted for more than 64% (64%−71%) of the total signal intensity of CHON−

591 compounds in the three cities (**Fig. 5g–i, l** and **Table S13**). The signal intensity

592 proportions of CHON− compounds formed by the ox_hy_N process in these three

593 cities (ranging from 47% in HZ to 69% in HEB) were higher than that in Wangdu (<

594 20%) (Jiang et al., 2023). The observation study in Wangdu examined aerosol organic

595 components only in ESI− mode (Jiang et al., 2023), which may underestimate the

596 importance of the CHO+ compounds that could serve as precursors of Ox-NOCs. In

597 general, CHON− compounds formed through the ox_hy_N and ox_N processes

598 showed the highest abundance in HEB, followed by BJ and HZ (**Fig. 5g–i**). According

599 to a simplified reaction mechanism for the formation of Ox-NOCs via aqueous-phase

600 processes (i.e., [Precursor] + [Oxidants] ↔ [Ox-NOCs]) (Shi et al., 2023; Kroflič et

601 al., 2015; Vione et al., 2005), we can infer that Ox-NOCs production is proportional

602 to precursor levels when oxidants (e.g., NO_2 radical or NO_2^+) are in a steady state in

603 the atmosphere. Indeed, the signal intensities of the Ox-CHON− compounds were

604 significantly positively correlated with the signal intensities of their CHO precursors

605 identified using the precursor-product pairs theory in HEB (**Fig. 6c**). Moreover, this

606 correlation gradually weakened from BJ to HZ (**Fig. 6c**). Thus, the spatial differences

607 in the contribution of the ox_hy_N and ox_N processes to Ox-NOC production across

608 the three cities can also be explained by differences in precursor emission intensity, as

609 indicated by above mentioned Re-NOC formation.

610

4. Conclusion

The abundance, composition, potential precursors, and potential formation mechanisms of NOCs in $PM_{2.5}$ in three Chinese cities with different energy consumption types during the winter were systematically investigated. On average, the total signal intensity of NOCs (i.e., CHN+, CHON+, and CHON− compounds) was highest in HEB, followed by BJ. The lowest total NOC signal intensity was found in HZ. According to the identification of potential precursors of NOCs, we found that anthropogenic aromatic compounds were the main precursors of NOCs during winter in HEB where mainly relies on coal for winter heating, with less impact from BVOCs. Anthropogenic aromatic precursors were also identified to be important contributors to NOC formation in BJ which uses natural gas and coal for winter heating, although the contribution ratio was lower in BJ than in HEB. In contrast, due to generally mild winters resulting in the absence of a winter heating policy and the implementation of strict pollution control measures, as mentioned previously, aromatic precursor emissions in HZ were expected to be the lowest. Furthermore, the NMDS analysis supported that the impact of anthropogenic fossil fuel combustion on NOC pollution gradually decreased from HEB to BJ and then to HZ.

The formation of CHON+ compounds was mainly associated with the cond_N, cond_hy_N, and cond_de_N processes. The cond_N and cond_de_N processes dominated the formation of CHN+ compounds. The production of CHON+ and

631   CHN+ compounds from the cond_N, cond_hy_N, and cond_de_N processes was

632   highest in HEB, followed by BJ and HZ. The ox_hy_N and ox_N processes

633   contributed significantly to CHON− compound formation, from which the highest

634   CHON− production occurred in HEB and the lowest in HZ. The spatial differences in

635   the contribution of different aqueous-phase processes to NOC production in the three

636   different cities can be attributed to differences in precursor emission intensity. In

637   particular, the contribution of these aqueous-phase processes to the formation of

638   CHON+ and CHN+ compounds showed the most significant increase from clean to

639   hazy days in HEB, followed by BJ. We concluded that high pollutant emission levels

640   can provide a greater potential to convert precursors to produce more NOCs via

641   aqueous-phase processes during haze periods. The above findings are summarized in

642   a diagram (**Fig. 7**).

643
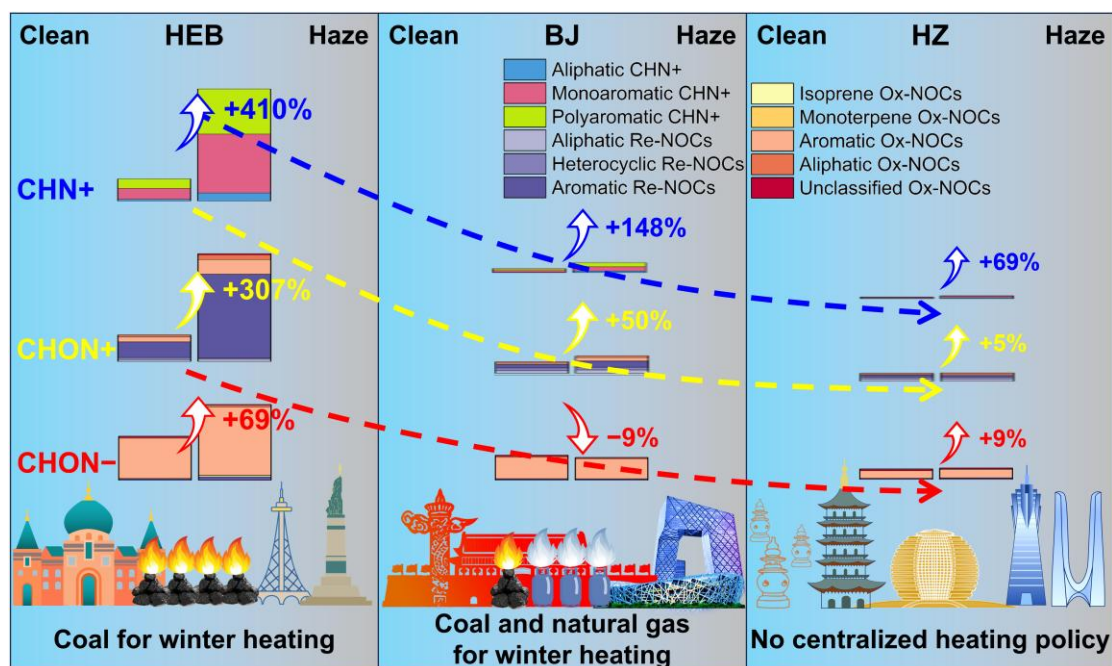
Figure 7. Conceptual illustration showing the characteristics of different NOCs from the clean days to the haze days in different cities.

In general, the aerosol NOCs pollution during winter is closely linked to both the intensity of precursor emissions and the efficiency of aqueous-phase processes in converting these emissions into NOCs. The overall results highlight the importance of emission reduction strategies in controlling aerosol NOCs pollution during winter. It is imperative to manage precursor emissions during hazy episodes in order to restrict the increased formation of secondary NOCs in conditions of high humidity. Moreover, targeted reduction of precursor emissions, especially from coal combustion, could significantly mitigate NOCs levels, thereby improving air quality and public health in urban areas. The transition to cleaner energy sources, as evidenced by the decreased gradient of NOC pollution from HEB to BJ to HZ, represents an effective pathway for the mitigation of NOC pollution. Future research should focus on further elucidating the specific pathways of aqueous-phase NOC formation and developing available models to predict NOC dynamics under varying environmental conditions. Additionally, research into the long-term effects of transitioning to cleaner energy sources on the reduction of NOC pollution will be essential for guiding effective air quality management strategies.

Data availability. The data presented in this work are available upon request from the

664   corresponding authors.

665

666   **Competing interests.** The authors declare no conflicts of interest relevant to this

667   study.

668

669   **Supplement.** Details of parameter calculation, classification method for identifying

670   precursors of NOCs, classification of possible aqueous-phase processes NOCs based

671   on precursor-product pairs, thirteen tables (Tables S1−S13), and fourteen extensive

672   figures (Figures S1−S14) are provided in the Supplement.

673

674   **Author contributions.** YX designed the study. YJM, TY, LG, HX, and HWX

675   performed field measurements and sample collection; YJM performed chemical

676   analysis; YX and YJM performed data analysis; YX and YJM wrote the original

677   manuscript; and YX, YJM, and HYX reviewed and edited the manuscript.

678

679   **Financial support.** This study was kindly supported by the National Natural Science

680   Foundation of China through grant 42303081, Shanghai "Science and Technology

681   Innovation Action Plan" Shanghai Sailing Program through grant 22YF1418700, and

682   the National Key Research and Development Program of China through gran

683   2023YFF0806001

684

685 **References**

686   Abudumutailifu, M., Shang, X., Wang, L., Zhang, M., Kang, H., Chen, Y., Li, L.,

687 Ju, R., Li, B., Ouyang, H., Tang, X., Li, C., Wang, L., Wang, X., George, C., Rudich,

688 Y., Zhang, R., and Chen, J.: Unveiling the Molecular Characteristics, Origins, and

689 Formation Mechanism of Reduced Nitrogen Organic Compounds in the Urban

690 Atmosphere of Shanghai Using a Versatile Aerosol Concentration Enrichment System,

691 Environ. Sci. Technol., 10.1021/acs.est.3c04071, 2024.

692   Arimoto, R., Duce, R. A., Savoie, D. L., Prospero, J. M., Talbot, R., Cullen, J. D.,

693 Tomza, U., Lewis, N. F., and Ray, B. J.: Relationships among aerosol constituents

694 from Asia and the North Pacific during PEM-West A, J. Geophys. Res.-Atmos., 101,

695 2011-2023, https://doi.org/10.1029/95JD01071, 1996.

696   Ayers, G. P. and Gras, J. L.: Seasonal relationship between cloud condensation

697 nuclei and aerosol methanesulphonate in marine air, Nature, 353, 834-835,

698 10.1038/353834a0, 1991.

699   Bond, T. C., Wehner, B., Plewka, A., Wiedensohler, A., Heintzenberg, J., and

700 Charlson, R. J.: Climate-relevant properties of primary particulate emissions from oil

701 and natural gas combustion, Atmos. Environ., 40, 3574-3587,

702 https://doi.org/10.1016/j.atmosenv.2005.12.030, 2006.

703   Cape, J. N., Cornell, S. E., Jickells, T. D., and Nemitz, E.: Organic nitrogen in

704   the atmosphere — Where does it come from? A review of sources and methods,

705   Atmos. Res., 102, 30-48, https://doi.org/10.1016/j.atmosres.2011.07.009, 2011.

706   Chao, A., Chazdon, R. L., Colwell, R. K., and Shen, T.-J.: Abundance-Based

707   Similarity Indices and Their Estimation When There Are Unseen Species in Samples,

708   Biometrics, 62, 361-371, https://doi.org/10.1111/j.1541-0420.2005.00489.x, 2006.

709   Chen, Y., Guo, H., Nah, T., Tanner, D. J., Sullivan, A. P., Takeuchi, M., Gao, Z.,

710   Vasilakos, P., Russell, A. G., Baumann, K., Huey, L. G., Weber, R. J., and Ng, N. L.:

711   Low-Molecular-Weight Carboxylic Acids in the Southeastern U.S.: Formation,

712   Partitioning, and Implications for Organic Aerosol Aging, Environ. Sci. Technol., 55,

713   6688-6699, 10.1021/acs.est.1c01413, 2021.

714   Chen, Z. M., Wang, H. L., Zhu, L. H., Wang, C. X., Jie, C. Y., and Hua, W.:

715   Aqueous-phase ozonolysis of methacrolein and methyl vinyl ketone: a potentially

716   important source of atmospheric aqueous oxidants, Atmos. Chem. Phys., 8, 2255-

717   2265, 10.5194/acp-8-2255-2008, 2008.

718   Ditto, J. C., Machesky, J., and Gentner, D. R.: Analysis of reduced and oxidized

719   nitrogen-containing organic compounds at a coastal site in summer and winter, Atmos.

720   Chem. Phys., 22, 3045-3065, https://doi.org/10.5194/acp-22-3045-2022, 2022.

721   Dong, P., Chen, Z., Qin, X., and Gong, Y.: Water Significantly Changes the Ring-

722   Cleavage Process During Aqueous Photooxidation of Toluene, Environ. Sci. Technol.,

723   55, 16316-16325, 10.1021/acs.est.1c04770, 2021.

724   Ehhalt, D. H. and Rohrer, F.: Dependence of the OH concentration on solar UV, J.

725   Geophys. Res.-Atmos., 105, 3565-3571, https://doi.org/10.1029/1999JD901070, 2000.

726   Gani, S., Bhandari, S., Seraj, S., Wang, D. S., Patel, K., Soni, P., Arub, Z., Habib,

727   G., Hildebrandt Ruiz, L., and Apte, J. S.: Submicron aerosol composition in the

728   world's most polluted megacity: the Delhi Aerosol Supersite study, Atmos. Chem.

729   Phys., 19, 6843-6859, 10.5194/acp-19-6843-2019, 2019.

730   Gao, J., Li, Y., Li, J., Shi, G., Liu, Z., Han, B., Tian, X., Wang, Y., Feng, Y., and

731   Russell, A. G.: Impact of Formation Pathways on Secondary Inorganic Aerosol

732   During Haze Pollution in Beijing: Quantitative Evidence From High-Resolution

733   Observation and Modeling, Geophys. Res. Lett., 48, e2021GL095623,

734   https://doi.org/10.1029/2021GL095623, 2021.

735   Gui, L., Xu, Y., You, Y.-C., Ma, Y.-J., Yang, T., Liu, T., Xiao, H.-W., Xiao, H.,

736   and Xiao, H.-Y.: Oxidative Degradation of Higher-Molecular-Weight Aromatic Amine

737   Compounds Is a Potential Source of Anilinium in Urban Aerosols, Environ. Sci.

738   Technol. Lett., 11, 1355-1361, 10.1021/acs.estlett.4c00935, 2024.

739   Guo, S., Hu, M., Zamora, M. L., Peng, J., Shang, D., Zheng, J., Du, Z., Wu, Z.,

740   Shao, M., Zeng, L., Molina, M. J., and Zhang, R.: Elucidating severe urban haze

741   formation in China, P. Natl. Acad. Sci. USA, 111, 17373-17378,

742   doi:10.1073/pnas.1419604111, 2014.

743   Guo, Y., Yan, C., Liu, Y., Qiao, X., Zheng, F., Zhang, Y., Zhou, Y., Li, C., Fan, X.,

744 Lin, Z., Feng, Z., Zhang, Y., Zheng, P., Tian, L., Nie, W., Wang, Z., Huang, D.,

745 Daellenbach, K. R., Yao, L., Dada, L., Bianchi, F., Jiang, J., Liu, Y., Kerminen, V. M.,

746 and Kulmala, M.: Seasonal variation in oxygenated organic molecules in urban

747 Beijing and their contribution to secondary organic aerosol, Atmos. Chem. Phys., 22,

748 10077-10097, 10.5194/acp-22-10077-2022, 2022.

749 Hallquist, M., Wenger, J. C., Baltensperger, U., Rudich, Y., Simpson, D., Claeys,

750 M., Dommen, J., Donahue, N. M., George, C., Goldstein, A. H., Hamilton, J. F.,

751 Herrmann, H., Hoffmann, T., Iinuma, Y., Jang, M., Jenkin, M. E., Jimenez, J. L.,

752 Kiendler-Scharr, A., Maenhaut, W., McFiggans, G., Mentel, T. F., Monod, A., Prévôt,

753 A. S. H., Seinfeld, J. H., Surratt, J. D., Szmigielski, R., and Wildt, J.: The formation,

754 properties and impact of secondary organic aerosol: current and emerging issues,

755 Atmos. Chem. Phys., 9, 5155-5236, 10.5194/acp-9-5155-2009, 2009.

756 Han, Y., Zhang, X., Li, L., Lin, Y., Zhu, C., Zhang, N., Wang, Q., and Cao, J.:

757 Enhanced Production of Organosulfur Species during a Severe Winter Haze Episode

758 in the Guanzhong Basin of Northwest China, Environ. Sci. Technol.,

759 https://doi.org/10.1021/acs.est.3c02914, 2023.

760 He, C., Che, H., Bao, Z., Liu, Y., Li, Q., Hu, M., Zhou, J., Zhang, S., Yao, X., Shi,

761 Q., Chen, C., Han, Y., Meng, L., Long, X., Yang, F., and Chen, Y.: Evolution of

762 nucleophilic high molecular-weight organic compounds in ambient aerosols: a case

763 study, Atmos. Chem. Phys., 24, 1627-1639, 10.5194/acp-24-1627-2024, 2024.

764   He, Q.-F., Ding, X., Fu, X.-X., Zhang, Y.-Q., Wang, J.-Q., Liu, Y.-X., Tang, M.-J.,

765   Wang, X.-M., and Rudich, Y.: Secondary Organic Aerosol Formation From Isoprene

766   Epoxides in the Pearl River Delta, South China: IEPOX- and HMML-Derived Tracers,

767   J. Geophys. Res.-Atmos., 123, 6999-7012, https://doi.org/10.1029/2017JD028242,

768   2018.

769   Heald, C. L., Kroll, J. H., Jimenez, J. L., Docherty, K. S., DeCarlo, P. F., Aiken,

770   A. C., Chen, Q., Martin, S. T., Farmer, D. K., and Artaxo, P.: A simplified description

771   of the evolution of organic aerosol composition in the atmosphere, Geophys. Res.

772   Lett., 37, https://doi.org/10.1029/2010GL042737, 2010.

773   Hodas, N., Sullivan, A. P., Skog, K., Keutsch, F. N., Collett, J. L., Jr., Decesari,

774   S., Facchini, M. C., Carlton, A. G., Laaksonen, A., and Turpin, B. J.: Aerosol Liquid

775   Water Driven by Anthropogenic Nitrate: Implications for Lifetimes of Water-Soluble

776   Organic Gases and Potential for Secondary Organic Aerosol Formation, Environ. Sci.

777   Technol., 48, 11127-11136, 10.1021/es5025096, 2014.

778   Huang, D., Zhang, X., Chen, Z. M., Zhao, Y., and Shen, X. L.: The kinetics and

779   mechanism of an aqueous phase isoprene reaction with hydroxyl radical, Atmos.

780   Chem. Phys., 11, 7399-7415, 10.5194/acp-11-7399-2011, 2011.

781   Huang, S., Shen, Z., Yang, X., Bai, G., Zhang, L., Zeng, Y., Sun, J., Xu, H., Ho,

782   S. S. H., Zhang, Y., and Cao, J.: Nitroaromatic compounds in six major Chinese cities:

783   Influence of different formation mechanisms on light absorption properties, Sci. Total

784   Environ., 930, 172672, https://doi.org/10.1016/j.scitotenv.2024.172672, 2024.

785   Jiang, H., Li, J., Tang, J., Zhao, S., Chen, Y., Tian, C., Zhang, X., Jiang, B., Liao,

786   Y., and Zhang, G.: Factors Influencing the Molecular Compositions and Distributions

787   of Atmospheric Nitrogen-Containing Compounds, J. Geophys. Res.-Atmos., 127,

788   e2021JD036284, https://doi.org/10.1029/2021JD036284, 2022.

789   Jiang, H., Cai, J., Feng, X., Chen, Y., Wang, L., Jiang, B., Liao, Y., Li, J., Zhang,

790   G., Mu, Y., and Chen, J.: Aqueous-Phase Reactions of Anthropogenic Emissions Lead

791   to the High Chemodiversity of Atmospheric Nitrogen-Containing Compounds during

792   the Haze Event, Environ. Sci. Technol., 57, 16500-16511, 10.1021/acs.est.3c06648,

793   2023.

794   Jimenez, N. G., Sharp, K. D., Gramyk, T., Ugland, D. Z., Tran, M.-K., Rojas, A.,

795   Rafla, M. A., Stewart, D., Galloway, M. M., Lin, P., Laskin, A., Cazaunau, M., Pangui,

796   E., Doussin, J.-F., and De Haan, D. O.: Radical-Initiated Brown Carbon Formation in

797   Sunlit Carbonyl–Amine–Ammonium Sulfate Mixtures and Aqueous Aerosol Particles,

798   ACS Earth Space Chem., 6, 228-238, 10.1021/acsearthspacechem.1c00395, 2022.

799   Kellerman, A. M., Dittmar, T., Kothawala, D. N., and Tranvik, L. J.:

800   Chemodiversity of dissolved organic matter in lakes driven by climate and hydrology,

801   Nature Communications, 5, 3804, 10.1038/ncomms4804, 2014.

802   Koch, B. P. and Dittmar, T.: From mass to structure: an aromaticity index for

803   high-resolution mass data of natural organic matter, Rapid Commun. Mass Spectrom.,

804   20, 926-932, https://doi.org/10.1002/rcm.2386, 2006.

805   Kroflič, A., Grilc, M., and Grgić, I.: Does toxicity of aromatic pollutants increase

806   under remote atmospheric conditions?, Scientific Reports, 5, 8859,

807   10.1038/srep08859, 2015.

808   Kroll, J. H., Donahue, N. M., Jimenez, J. L., Kessler, S. H., Canagaratna, M. R.,

809   Wilson, K. R., Altieri, K. E., Mazzoleni, L. R., Wozniak, A. S., Bluhm, H., Mysak, E.

810   R., Smith, J. D., Kolb, C. E., and Worsnop, D. R.: Carbon oxidation state as a metric

811   for describing the chemistry of atmospheric organic aerosol, Nat. Chem., 3, 133-139,

812   https://doi.org/10.1038/nchem.948, 2011.

813   Křůmal, K., Mikuška, P., Horák, J., Hopan, F., and Krpec, K.: Comparison of

814   emissions of gaseous and particulate pollutants from the combustion of biomass and

815   coal in modern and old-type boilers used for residential heating in the Czech Republic,

816   Central   Europe,   Chemosphere,   229,   51-59,

817   https://doi.org/10.1016/j.chemosphere.2019.04.137, 2019.

818   Kuwata, M. and Martin, S. T.: Phase of atmospheric secondary organic material

819   affects   its   reactivity,   P.   Natl.   Acad.   Sci.   USA,   109,   17354-17359,

820   doi:10.1073/pnas.1209071109, 2012.

821   Laskin, J., Laskin, A., Nizkorodov, S. A., Roach, P., Eckert, P., Gilles, M. K.,

822   Wang, B., Lee, H. J., and Hu, Q.: Molecular Selectivity of Brown Carbon

823   Chromophores,   Environ.   Sci.   Technol.,   48,   12047-12055,

824   https://doi.org/10.1021/es503432r, 2014.

825   Lee, A. K. Y., Zhao, R., Li, R., Liggio, J., Li, S.-M., and Abbatt, J. P. D.:

826   Formation of Light Absorbing Organo-Nitrogen Species from Evaporation of

827   Droplets Containing Glyoxal and Ammonium Sulfate, Environ. Sci. Technol., 47,

828   12819-12826, 10.1021/es402687w, 2013.

829   Li, X., Song, S., Zhou, W., Hao, J., Worsnop, D. R., and Jiang, J.: Interactions

830   between aerosol organic components and liquid water content during haze episodes in

831   Beijing, Atmos. Chem. Phys., 19, 12163-12174, 10.5194/acp-19-12163-2019, 2019a.

832   Li, Y., Fu, T.-M., Yu, J. Z., Yu, X., Chen, Q., Miao, R., Zhou, Y., Zhang, A., Ye, J.,

833   Yang, X., Tao, S., Liu, H., and Yao, W.: Dissecting the contributions of organic

834   nitrogen aerosols to global atmospheric nitrogen deposition and implications for

835   ecosystems, National Science Review, 10, 10.1093/nsr/nwad244, 2023.

836   Li, Z., Nizkorodov, S. A., Chen, H., Lu, X., Yang, X., and Chen, J.: Nitrogen-

837   containing secondary organic aerosol formation by acrolein reaction with

838   ammonia/ammonium, Atmos. Chem. Phys., 19, 1343-1356, 10.5194/acp-19-1343-

839   2019, 2019b.

840   Lian, L., Yan, S., Zhou, H., and Song, W.: Overview of the Phototransformation

841   of Wastewater Effluents by High-Resolution Mass Spectrometry, Environ. Sci.

842   Technol., 54, 1816-1826, 10.1021/acs.est.9b04669, 2020.

843   Lin, X., Xu, Y., Zhu, R.-G., Xiao, H.-W., and Xiao, H.-Y.: Proteinaceous Matter

844   in $PM_{2.5}$ in Suburban Guiyang, Southwestern China: Decreased Importance in Long-

845   Range Transport and Atmospheric Degradation, J. Geophys. Res.-Atmos., 128,

846   e2023JD038516, https://doi.org/10.1029/2023JD038516, 2023.

847   Liu, T., Xu, Y., Sun, Q.-B., Xiao, H.-W., Zhu, R.-G., Li, C.-X., Li, Z.-Y., Zhang,

848   K.-Q., Sun, C.-X., and Xiao, H.-Y.: Characteristics, Origins, and Atmospheric

849   Processes of Amines in Fine Aerosol Particles in Winter in China, J. Geophys. Res.-

850   Atmos., 128, e2023JD038974, https://doi.org/10.1029/2023JD038974, 2023a.

851   Liu, X.-Y., He, K.-B., Zhang, Q., Lu, Z.-F., Wang, S.-W., Zhang, Y.-X., and

852   Streets, D. G.: Analysis of the origins of black carbon and carbon monoxide

853   transported to Beijing, Tianjin, and Hebei in China, Sci. Total Environ., 653, 1364-

854   1376, https://doi.org/10.1016/j.scitotenv.2018.09.274, 2019.

855   Liu, X., Wang, H., Wang, F., Lv, S., Wu, C., Zhao, Y., Zhang, S., Liu, S., Xu, X.,

856   Lei, Y., and Wang, G.: Secondary Formation of Atmospheric Brown Carbon in China

857   Haze: Implication for an Enhancing Role of Ammonia, Environ. Sci. Technol., 57,

858   11163-11172, 10.1021/acs.est.3c03948, 2023b.

859   Liu, Y., Nie, W., Li, Y., Ge, D., Liu, C., Xu, Z., Chen, L., Wang, T., Wang, L.,

860   Sun, P., Qi, X., Wang, J., Xu, Z., Yuan, J., Yan, C., Zhang, Y., Huang, D., Wang, Z.,

861   Donahue, N. M., Worsnop, D., Chi, X., Ehn, M., and Ding, A.: Formation of

862   condensable organic vapors from anthropogenic and biogenic volatile organic

863   compounds (VOCs) is strongly perturbed by NOx in eastern China, Atmos. Chem.

864 Phys., 21, 14789-14814, 10.5194/acp-21-14789-2021, 2021.

865 Liu, Z., Zhu, B., Zhu, C., Ruan, T., Li, J., Chen, H., Li, Q., Wang, X., Wang, L.,

866 Mu, Y., Collett, J., George, C., Wang, Y., Wang, X., Su, J., Yu, S., Mellouki, A., Chen,

867 J., and Jiang, G.: Abundant nitrogenous secondary organic aerosol formation

868 accelerated by cloud processing, iScience, 26, 108317,

869 https://doi.org/10.1016/j.isci.2023.108317, 2023c.

870 Lv, S., Wang, F., Wu, C., Chen, Y., Liu, S., Zhang, S., Li, D., Du, W., Zhang, F.,

871 Wang, H., Huang, C., Fu, Q., Duan, Y., and Wang, G.: Gas-to-Aerosol Phase

872 Partitioning of Atmospheric Water-Soluble Organic Compounds at a Rural Site in

873 China: An Enhancing Effect of NH_3 on SOA Formation, Environ. Sci. Technol., 56,

874 3915-3924, 10.1021/acs.est.1c06855, 2022.

875 Ma, L., Li, B., Liu, Y., Sun, X., Fu, D., Sun, S., Thapa, S., Geng, J., Qi, H.,

876 Zhang, A., and Tian, C.: Characterization, sources and risk assessment of $PM_{2.5}$-bound

877 polycyclic aromatic hydrocarbons (PAHs) and nitrated PAHs (NPAHs) in Harbin, a

878 cold city in Northern China, Journal of Cleaner Production, 264, 121673,

879 https://doi.org/10.1016/j.jclepro.2020.121673, 2020.

880 Ma, Y. J., Xu, Y., Yang, T., Xiao, H. W., and Xiao, H. Y.: Measurement report:

881 Characteristics of nitrogen-containing organics in $PM_{2.5}$ in Ürümqi, northwestern

882 China – differential impacts of combustion of fresh and aged biomass materials,

883 Atmos. Chem. Phys., 24, 4331-4346, 10.5194/acp-24-4331-2024, 2024.

884   Mafusire, G., Annegarn, H. J., Vakkari, V., Beukes, J. P., Josipovic, M., van Zyl,

885   P. G., and Laakso, L.: Submicrometer aerosols and excess CO as tracers for biomass

886   burning air mass transport over southern Africa, J. Geophys. Res.-Atmos., 121,

887   10,262-210,282, https://doi.org/10.1002/2015JD023965, 2016.

888   MEEPRC: Technical Regulation on Ambient Air Quality Index (on trial): HJ

889   633—2012, Ministry of Ecology and Environment of the People's Republic of China,

890   https://www.mee.gov.cn/ywgz/fgbz/bz/bzwb/jcffbz/201203/t20120302_224166.shtml,

891   (last access: 10 December 2024), 2012.

892   Montoya-Aguilera, J., Hinks, M. L., Aiona, P. K., Wingen, L. M., Horne, J. R.,

893   Zhu, S., Dabdub, D., Laskin, A., Laskin, J., Lin, P., and Nizkorodov, S. A.: Reactive

894   Uptake of Ammonia by Biogenic and Anthropogenic Organic Aerosols, in:

895   Multiphase Environmental Chemistry in the Atmosphere, ACS Symposium Series,

896   1299, American Chemical Society, 127-147, doi:10.1021/bk-2018-1299.ch007

897   10.1021/bk-2018-1299.ch007, 2018.

898   Ng, N. L., Brown, S. S., Archibald, A. T., Atlas, E., Cohen, R. C., Crowley, J. N.,

899   Day, D. A., Donahue, N. M., Fry, J. L., Fuchs, H., Griffin, R. J., Guzman, M. I.,

900   Herrmann, H., Hodzic, A., Iinuma, Y., Jimenez, J. L., Kiendler-Scharr, A., Lee, B. H.,

901   Luecken, D. J., Mao, J., McLaren, R., Mutzel, A., Osthoff, H. D., Ouyang, B.,

902   Picquet-Varrault, B., Platt, U., Pye, H. O. T., Rudich, Y., Schwantes, R. H., Shiraiwa,

903   M., Stutz, J., Thornton, J. A., Tilgner, A., Williams, B. J., and Zaveri, R. A.: Nitrate

904 radicals and biogenic volatile organic compounds: oxidation, mechanisms, and

905 organic aerosol, Atmos. Chem. Phys., 17, 2103-2162, 10.5194/acp-17-2103-2017,

906 2017.

907 Nguyen, T. B., Bates, K. H., Crounse, J. D., Schwantes, R. H., Zhang, X.,

908 Kjaergaard, H. G., Surratt, J. D., Lin, P., Laskin, A., Seinfeld, J. H., and Wennberg, P.

909 O.: Mechanism of the hydroxyl radical oxidation of methacryloyl peroxynitrate

910 (MPAN) and its pathway toward secondary organic aerosol formation in the

911 atmosphere, Phys. Chem. Chem. Phys., 17, 17914-17926,

912 https://doi.org/10.1039/C5CP02001H, 2015.

913 Nie, W., Yan, C., Huang, D. D., Wang, Z., Liu, Y., Qiao, X., Guo, Y., Tian, L.,

914 Zheng, P., Xu, Z., Li, Y., Xu, Z., Qi, X., Sun, P., Wang, J., Zheng, F., Li, X., Yin, R.,

915 Dallenbach, K. R., Bianchi, F., Petäjä, T., Zhang, Y., Wang, M., Schervish, M., Wang,

916 S., Qiao, L., Wang, Q., Zhou, M., Wang, H., Yu, C., Yao, D., Guo, H., Ye, P., Lee, S.,

917 Li, Y. J., Liu, Y., Chi, X., Kerminen, V.-M., Ehn, M., Donahue, N. M., Wang, T.,

918 Huang, C., Kulmala, M., Worsnop, D., Jiang, J., and Ding, A.: Secondary organic

919 aerosol formed by condensing anthropogenic vapours over China's megacities, Nature

920 Geoscience, 15, 255-261, 10.1038/s41561-022-00922-5, 2022.

921 Nozière, B., Kalberer, M., Claeys, M., Allan, J., D'Anna, B., Decesari, S.,

922 Finessi, E., Glasius, M., Grgić, I., Hamilton, J. F., Hoffmann, T., Iinuma, Y., Jaoui, M.,

923 Kahnt, A., Kampf, C. J., Kourtchev, I., Maenhaut, W., Marsden, N., Saarikoski, S.,

924 Schnelle-Kreis, J., Surratt, J. D., Szidat, S., Szmigielski, R., and Wisthaler, A.: The

925 Molecular Identification of Organic Compounds in the Atmosphere: State of the Art

926 and Challenges, Chem. Rev., 115, 3919-3983, 10.1021/cr5003485, 2015.

927 Oksanen, J., Kindt, R., Legendre, P., O'Hara, B., Stevens, M. H. H., Oksanen, M.

928 J., and Suggests, M.: The vegan package, Community ecology package, 10, 719, 2007.

929 Perraud, V., Bruns, E. A., Ezell, M. J., Johnson, S. N., Yu, Y., Alexander, M. L.,

930 Zelenyuk, A., Imre, D., Chang, W. L., Dabdub, D., Pankow, J. F., and Finlayson-Pitts,

931 B. J.: Nonequilibrium atmospheric secondary organic aerosol formation and growth, P.

932 Natl. Acad. Sci. USA, 109, 2836-2841, doi:10.1073/pnas.1119909109, 2012.

933 Rollins, A. W., Browne, E. C., Min, K.-E., Pusede, S. E., Wooldridge, P. J.,

934 Gentner, D. R., Goldstein, A. H., Liu, S., Day, D. A., Russell, L. M., and Cohen, R. C.:

935 Evidence for NO_x Control over Nighttime SOA Formation, Science, 337, 1210-1212,

936 https://doi.org/10.1126/science.1221520, 2012.

937 Shen, Z., Cao, J., Arimoto, R., Han, Z., Zhang, R., Han, Y., Liu, S., Okuda, T.,

938 Nakao, S., and Tanaka, S.: Ionic composition of TSP and $PM_{2.5}$ during dust storms

939 and air pollution episodes at Xi'an, China, Atmos. Environ., 43, 2911-2918,

940 https://doi.org/10.1016/j.atmosenv.2009.03.005, 2009.

941 Shi, X., Qiu, X., Cheng, Z., Chen, Q., Rudich, Y., and Zhu, T.: Isomeric

942 Identification of Particle-Phase Organic Nitrates through Gas Chromatography and

943 Time-of-Flight Mass Spectrometry Coupled with an Electron Capture Negative

944 Ionization Source, Environ. Sci. Technol., 54, 707-713, 10.1021/acs.est.9b05818,

945 2020.

946 Shi, X., Qiu, X., Li, A., Jiang, X., Wei, G., Zheng, Y., Chen, Q., Chen, S., Hu, M.,

947 Rudich, Y., and Zhu, T.: Polar Nitrated Aromatic Compounds in Urban Fine

948 Particulate Matter: A Focus on Formation via an Aqueous-Phase Radical Mechanism,

949 Environ. Sci. Technol., 57, 5160-5168, 10.1021/acs.est.2c07324, 2023.

950 Singh, S. and Kumar, R.: Air Pollution and Its Associated Impacts on

951 Atmosphere and Biota Health, in: Extremes in Atmospheric Processes and

952 Phenomenon: Assessment, Impacts and Mitigation, edited by: Saxena, P., Shukla, A.,

953 and Gupta, A. K., Springer Nature Singapore, Singapore, 29-58, 10.1007/978-981-16-

954 7727-4_3, 2022.

955 Song, J., Li, M., Jiang, B., Wei, S., Fan, X., and Peng, P. a.: Molecular

956 Characterization of Water-Soluble Humic like Substances in Smoke Particles Emitted

957 from Combustion of Biomass Materials and Coal Using Ultrahigh-Resolution

958 Electrospray Ionization Fourier Transform Ion Cyclotron Resonance Mass

959 Spectrometry, Environ. Sci. Technol., 52, 2575-2585,

960 https://doi.org/10.1021/acs.est.7b06126, 2018.

961 Song, J., Li, M., Zou, C., Cao, T., Fan, X., Jiang, B., Yu, Z., Jia, W., and Peng, P.

962 a.: Molecular Characterization of Nitrogen-Containing Compounds in Humic-like

963 Substances Emitted from Biomass Burning and Coal Combustion, Environ. Sci.

964 Technol., 56, 119-130, https://doi.org/10.1021/acs.est.1c04451, 2022.

965 Stockwell, C. E., Veres, P. R., Williams, J., and Yokelson, R. J.: Characterization

966 of biomass burning emissions from cooking fires, peat, crop residue, and other fuels

967 with high-resolution proton-transfer-reaction time-of-flight mass spectrometry, Atmos.

968 Chem. Phys., 15, 845-865, 10.5194/acp-15-845-2015, 2015.

969 Streets, D. G. and Waldhoff, S. T.: Present and future emissions of air pollutants

970 in China:: SO_2, NO_x, and CO, Atmos. Environ., 34, 363-374,

971 https://doi.org/10.1016/S1352-2310(99)00167-3, 2000.

972 Su, S., Xie, Q., Lang, Y., Cao, D., Xu, Y., Chen, J., Chen, S., Hu, W., Qi, Y., Pan,

973 X., Sun, Y., Wang, Z., Liu, C.-Q., Jiang, G., and Fu, P.: High Molecular Diversity of

974 Organic Nitrogen in Urban Snow in North China, Environ. Sci. Technol., 55, 4344-

975 4356, https://dx.doi.org/10.1021/acs.est.0c06851, 2021.

976 Suess, E., Aemisegger, F., Sonke, J. E., Sprenger, M., Wernli, H., and Winkel, L.

977 H. E.: Marine versus Continental Sources of Iodine and Selenium in Rainfall at Two

978 European High-Altitude Locations, Environ. Sci. Technol., 53, 1905-1917,

979 10.1021/acs.est.8b05533, 2019.

980 Sun, W., Hu, X., Fu, Y., Zhang, G., Zhu, Y., Wang, X., Yan, C., Xue, L., Meng,

981 H., Jiang, B., Liao, Y., Wang, X., Peng, P., and Bi, X.: Different formation pathways

982 of nitrogen-containing organic compounds in aerosols and fog water in northern

983 China, Atmos. Chem. Phys., 24, 6987-6999, 10.5194/acp-24-6987-2024, 2024.

984   Surratt, J. D., Chan, A. W. H., Eddingsaas, N. C., Chan, M., Loza, C. L., Kwan,

985 A. J., Hersey, S. P., Flagan, R. C., Wennberg, P. O., and Seinfeld, J. H.: Reactive

986 intermediates revealed in secondary organic aerosol formation from isoprene, P. Natl.

987 Acad. Sci. USA, 107, 6640-6645, doi:10.1073/pnas.0911114107, 2010.

988   Vione, D., Maurino, V., Minero, C., and Pelizzetti, E.: Aqueous Atmospheric

989 Chemistry: Formation of 2,4-Dinitrophenol upon Nitration of 2-Nitrophenol and 4-

990 Nitrophenol in Solution, Environ. Sci. Technol., 39, 7921-7931, 10.1021/es050824m,

991 2005.

992   Vu, T. V., Shi, Z., Cheng, J., Zhang, Q., He, K., Wang, S., and Harrison, R. M.:

993 Assessing the impact of clean air action on air quality trends in Beijing using a

994 machine learning technique, Atmos. Chem. Phys., 19, 11303-11314, 10.5194/acp-19-

995 11303-2019, 2019.

996   Wang, D., Shen, Z., Yang, X., Huang, S., Luo, Y., Bai, G., and Cao, J.: Insight

997 into the Role of NH_3/NH_4^+ and NO_x/NO_3^- in the Formation of Nitrogen-Containing

998 Brown Carbon in Chinese Megacities, Environ. Sci. Technol., 58, 4281-4290,

999 10.1021/acs.est.3c10374, 2024.

1000   Wang, J., Sun, S., Zhang, C., Xue, C., Liu, P., Zhang, C., Mu, Y., Wu, H., Wang,

1001 D., Chen, H., and Chen, J.: The pollution levels, variation characteristics, sources and

1002 implications of atmospheric carbonyls in a typical rural area of North China Plain

1003 during winter, Journal of Environmental Sciences, 95, 256-265,

1004   https://doi.org/10.1016/j.jes.2020.05.003, 2020.

1005   Wang, J., Ye, J., Zhang, Q., Zhao, J., Wu, Y., Li, J., Liu, D., Li, W., Zhang, Y.,

1006   Wu, C., Xie, C., Qin, Y., Lei, Y., Huang, X., Guo, J., Liu, P., Fu, P., Li, Y., Lee, H. C.,

1007   Choi, H., Zhang, J., Liao, H., Chen, M., Sun, Y., Ge, X., Martin, S. T., and Jacob, D. J.:

1008   Aqueous production of secondary organic aerosol from fossil-fuel emissions in winter

1009   Beijing   haze,   P.   Natl.   Acad.   Sci.   USA,   118,   e2022179118,

1010   doi:10.1073/pnas.2022179118, 2021a.

1011   Wang, K., Zhang, Y., Huang, R.-J., Cao, J., and Hoffmann, T.: UHPLC-Orbitrap

1012   mass spectrometric characterization of organic aerosol from a central European city

1013   (Mainz, Germany) and a Chinese megacity (Beijing), Atmos. Environ., 189, 22-29,

1014   https://doi.org/10.1016/j.atmosenv.2018.06.036, 2018.

1015   Wang, K., Huang, R.-J., Brueggemand, M., Zhang, Y., Yang, L., Ni, H., Guo, J.,

1016   Wang, M., Han, J., Bilde, M., Glasius, M., and Hoffmann, T.: Urban organic aerosol

1017   composition in eastern China differs from north to south: molecular insight from a

1018   liquid chromatography-mass spectrometry (Orbitrap) study, Atmos. Chem. Phys., 21,

1019   9089-9104, https://doi.org/10.5194/acp-21-9089-2021, 2021b.

1020   Wang, Y., Zhao, Y., Li, Z., Li, C., Yan, N., and Xiao, H.: Importance of Hydroxyl

1021   Radical Chemistry in Isoprene Suppression of Particle Formation from α-Pinene

1022   Ozonolysis,   ACS   Earth   Space   Chem.,   5,   487-499,

1023   https://doi.org/10.1021/acsearthspacechem.0c00294, 2021c.

1024   Wang, Y., Zhuang, G., Zhang, X., Huang, K., Xu, C., Tang, A., Chen, J., and An,

1025   Z.: The ion chemistry, seasonal cycle, and sources of $PM_{2.5}$ and TSP aerosol in

1026   Shanghai, Atmos. Environ., 40, 2935-2952,

1027   https://doi.org/10.1016/j.atmosenv.2005.12.051, 2006.

1028   Wang, Y., Hu, M., Lin, P., Guo, Q., Wu, Z., Li, M., Zeng, L., Song, Y., Zeng, L.,

1029   Wu, Y., Guo, S., Huang, X., and He, L.: Molecular Characterization of Nitrogen-

1030   Containing Organic Compounds in Humic-like Substances Emitted from Straw

1031   Residue Burning, Environ. Sci. Technol., 51, 5951-5961,

1032   https://doi.org/10.1021/acs.est.7b00248, 2017.

1033   Wang, Y., Hu, M., Hu, W., Zheng, J., Niu, H., Fang, X., Xu, N., Wu, Z., Guo, S.,

1034   Wu, Y., Chen, W., Lu, S., Shao, M., Xie, S., Luo, B., and Zhang, Y.: Secondary

1035   Formation of Aerosols Under Typical High-Humidity Conditions in Wintertime

1036   Sichuan Basin, China: A Contrast to the North China Plain, J. Geophys. Res.-Atmos.,

1037   126, e2021JD034560, https://doi.org/10.1029/2021JD034560, 2021d.

1038   Wen, W., Shi, L., Li, L., Wang, L., and Chen, J.: Molecular characteristics of

1039   ambient organic aerosols in Shanghai winter before and after the COVID-19 outbreak,

1040   Sci. Total Environ., 869, 161811, https://doi.org/10.1016/j.scitotenv.2023.161811,

1041   2023.

1042   Wu, Z., Wang, Y., Tan, T., Zhu, Y., Li, M., Shang, D., Wang, H., Lu, K., Guo, S.,

1043   Zeng, L., and Zhang, Y.: Aerosol Liquid Water Driven by Anthropogenic Inorganic

1044 Salts: Implying Its Key Role in Haze Formation over the North China Plain, Environ.

1045 Sci. Technol. Lett., 5, 160-166, 10.1021/acs.estlett.8b00021, 2018.

1046  Xi, Y., Wang, Q., Zhu, J., Yang, M., Hao, T., Chen, Y., Zhang, Q., He, N., and Yu,

1047 G.: Atmospheric wet organic nitrogen deposition in China: Insights from the national

1048 observation network, Sci. Total Environ., 898, 165629,

1049 https://doi.org/10.1016/j.scitotenv.2023.165629, 2023.

1050  Xiao, H.-Y. and Liu, C.-Q.: Chemical characteristics of water-soluble

1051 components in TSP over Guiyang, SW China, 2003, Atmos. Environ., 38, 6297-6306,

1052 https://doi.org/10.1016/j.atmosenv.2004.08.033, 2004.

1053  Xu, B., Zhang, G., Gustafsson, Ö., Kawamura, K., Li, J., Andersson, A., Bikkina,

1054 S., Kunwar, B., Pokhrel, A., Zhong, G., Zhao, S., Li, J., Huang, C., Cheng, Z., Zhu, S.,

1055 Peng, P., and Sheng, G.: Large contribution of fossil-derived components to aqueous

1056 secondary organic aerosols in China, Nature Communications, 13, 5115,

1057 10.1038/s41467-022-32863-3, 2022a.

1058  Xu, Y., Xiao, H., Wu, D., and Long, C.: Abiotic and Biological Degradation of

1059 Atmospheric Proteinaceous Matter Can Contribute Significantly to Dissolved Amino

1060 Acids in Wet Deposition, Environ. Sci. Technol., 54, 6551-6561,

1061 10.1021/acs.est.0c00421, 2020a.

1062  Xu, Y., Dong, X.-N., Xiao, H.-Y., He, C., and Wu, D.-S.: Water-Insoluble

1063 Components in Rainwater in Suburban Guiyang, Southwestern China: A Potential

Contributor to Dissolved Organic Carbon, J. Geophys. Res.-Atmos., 127, e2022JD037721, https://doi.org/10.1029/2022JD037721, 2022b.

Xu, Y., Dong, X.-N., Xiao, H.-Y., Zhou, J.-X., and Wu, D.-S.: Proteinaceous Matter and Liquid Water in Fine Aerosols in Nanchang, Eastern China: Seasonal Variations, Sources, and Potential Connections, J. Geophys. Res.-Atmos., 127, e2022JD036589, https://doi.org/10.1029/2022JD036589, 2022c.

Xu, Y., Dong, X. N., He, C., Wu, D. S., Xiao, H. W., and Xiao, H. Y.: Mist cannon trucks can exacerbate the formation of water-soluble organic aerosol and $PM_{2.5}$ pollution in the road environment, Atmos. Chem. Phys., 23, 6775-6788, https://doi.org/10.5194/acp-23-6775-2023, 2023.

Xu, Y., Lin, X., Sun, Q.-B., Xiao, H.-W., Xiao, H., and Xiao, H.-Y.: Elaborating the Atmospheric Transformation of Combined and Free Amino Acids From the Perspective of Observational Studies, J. Geophys. Res.-Atmos., 129, e2024JD040730, https://doi.org/10.1029/2024JD040730, 2024a.

Xu, Y., Liu, T., Ma, Y. J., Sun, Q. B., Xiao, H. W., Xiao, H., Xiao, H. Y., and Liu, C. Q.: Measurement report: Occurrence of aminiums in PM2.5 during winter in China – aminium outbreak during polluted episodes and potential constraints, Atmos. Chem. Phys., 24, 10531-10542, 10.5194/acp-24-10531-2024, 2024b.

Xu, Y., Miyazaki, Y., Tachibana, E., Sato, K., Ramasamy, S., Mochizuki, T., Sadanaga, Y., Nakashima, Y., Sakamoto, Y., Matsuda, K., and Kajii, Y.: Aerosol

1084   Liquid Water Promotes the Formation of Water-Soluble Organic Nitrogen in

1085   Submicrometer Aerosols in a Suburban Forest, Environ. Sci. Technol., 54, 1406-1414,

1086   https://dx.doi.org/10.1021/acs.est.9b05849, 2020b.

1087   Yan, F., Su, H., Cheng, Y., Huang, R., Liao, H., Yang, T., Zhu, Y., Zhang, S.,

1088   Sheng, L., Kou, W., Zeng, X., Xiang, S., Yao, X., Gao, H., and Gao, Y.: Frequent haze

1089   events associated with transport and stagnation over the corridor between the North

1090   China Plain and Yangtze River Delta, Atmos. Chem. Phys., 24, 2365-2376,

1091   10.5194/acp-24-2365-2024, 2024.

1092   Yang, L., Huang, R.-J., Yuan, W., Huang, D. D., and Huang, C.: pH-Dependent

1093   Aqueous-Phase Brown Carbon Formation: Rate Constants and Implications for Solar

1094   Absorption and Atmospheric Photochemistry, Environ. Sci. Technol., 58, 1236-1243,

1095   10.1021/acs.est.3c07631, 2024a.

1096   Yang, T., Xu, Y., Ma, Y.-J., Wang, Y.-C., Yu, J. Z., Sun, Q.-B., Xiao, H.-W., Xiao,

1097   H.-Y., and Liu, C.-Q.: Field Evidence for Constraints of Nearly Dry and Weakly

1098   Acidic Aerosol Conditions on the Formation of Organosulfates, Environ. Sci. Technol.

1099   Lett., 11, 981-987, 10.1021/acs.estlett.4c00522, 2024b.

1100   Yang, T., Xu, Y., Ye, Q., Ma, Y. J., Wang, Y. C., Yu, J. Z., Duan, Y. S., Li, C. X.,

1101   Xiao, H. W., Li, Z. Y., Zhao, Y., and Xiao, H. Y.: Spatial and diurnal variations of

1102   aerosol organosulfates in summertime Shanghai, China: potential influence of

1103   photochemical processes and anthropogenic sulfate pollution, Atmos. Chem. Phys., 23,

1104   13433-13450, https://doi.org/10.5194/acp-23-13433-2023, 2023.

1105   Yang, X., Huang, S., Li, D., Xu, H., Zeng, Y., Yang, L., Wang, D., Zhang, N.,

1106 Cao, J., and Shen, Z.: Water-soluble organic matter with various polarities in PM2.5

1107 over Xi'an, China: Abundance, functional groups, and light absorption, Particuology,

1108 84, 281-289, https://doi.org/10.1016/j.partic.2023.07.005, 2024c.

1109   Yassine, M. M., Harir, M., Dabek-Zlotorzynska, E., and Schmitt-Kopplin, P.:

1110 Structural characterization of organic aerosol using Fourier transform ion cyclotron

1111 resonance mass spectrometry: Aromaticity equivalent approach, Rapid Commun.

1112 Mass Spectrom., 28, 2445-2454, https://doi.org/10.1002/rcm.7038, 2014.

1113   Yu, X., Pan, Y., Song, W., Li, S., Li, D., Zhu, M., Zhou, H., Zhang, Y., Li, D., Yu,

1114 J., Wang, X., and Wang, X.: Wet and Dry Nitrogen Depositions in the Pearl River

1115 Delta, South China: Observations at Three Typical Sites With an Emphasis on Water-

1116 Soluble Organic Nitrogen, J. Geophys. Res.-Atmos., 125, e2019JD030983,

1117 https://doi.org/10.1029/2019JD030983, 2020.

1118   Yuan, W., Huang, R.-J., Shen, J., Wang, K., Yang, L., Wang, T., Gong, Y., Cao,

1119 W., Guo, J., Ni, H., Duan, J., and Hoffmann, T.: More water-soluble brown carbon

1120 after the residential "coal-to-gas" conversion measure in urban Beijing, npj Climate

1121 and Atmospheric Science, 6, 20, 10.1038/s41612-023-00355-w, 2023.

1122   Zeng, Y., Ning, Y., Shen, Z., Zhang, L., Zhang, T., Lei, Y., Zhang, Q., Li, G., Xu,

1123 H., Ho, S. S. H., and Cao, J.: The Roles of N, S, and O in Molecular Absorption

1124 Features of Brown Carbon in $PM_{2.5}$ in a Typical Semi-Arid Megacity in Northwestern

1125 China, J. Geophys. Res.-Atmos., 126, e2021JD034791,

1126 https://doi.org/10.1029/2021JD034791, 2021.

1127 Zhang, B., Shen, Z., He, K., Zhang, L., Huang, S., Sun, J., Xu, H., Li, J., Yang,

1128 L., and Cao, J.: Source Profiles of Particle-Bound Phenolic Compounds and Aromatic

1129 Acids From Fresh and Aged Solid Fuel Combustion: Implication for the Aging

1130 Mechanism and Newly Proposed Source Tracers, J. Geophys. Res.-Atmos., 128,

1131 e2023JD039758, https://doi.org/10.1029/2023JD039758, 2023a.

1132 Zhang, H., He, P., Liu, L., Dai, H., Zhao, B., Zeng, Y., Bi, J., Liu, M., and Ji, J. S.:

1133 Trade-offs between cold protection and air pollution–induced mortality of China's

1134 heating policy, PNAS Nexus, 2, 10.1093/pnasnexus/pgad387, 2023b.

1135 Zhang, T., Cao, J. J., Tie, X. X., Shen, Z. X., Liu, S. X., Ding, H., Han, Y. M.,

1136 Wang, G. H., Ho, K. F., Qiang, J., and Li, W. T.: Water-soluble ions in atmospheric

1137 aerosols measured in Xi'an, China: Seasonal variations and sources, Atmos. Res., 102,

1138 110-119, https://doi.org/10.1016/j.atmosres.2011.06.014, 2011.

1139 Zhang, Y.-L. and Cao, F.: Fine particulate matter ($PM_{2.5}$) in China at a city level,

1140 Scientific Reports, 5, 14884, 10.1038/srep14884, 2015.

1141 Zhang, Z., Guan, H., Xiao, H., Liang, Y., Zheng, N., Luo, L., Liu, C., Fang, X.,

1142 and Xiao, H.: Oxidation and sources of atmospheric NO_x during winter in Beijing

1143 based on $\delta^{18}O$-$\delta^{15}N$ space of particulate nitrate, Environmental Pollution, 276, 116708,

1144 https://doi.org/10.1016/j.envpol.2021.116708, 2021a.

1145 Zhang, Z., Zhou, Y., Zhao, N., Li, H., Tohniyaz, B., Mperejekumana, P., Hong,

1146 Q., Wu, R., Li, G., Sultan, M., Zayan, A. M. I., Cao, J., Ahmad, R., and Dong, R.:

1147 Clean heating during winter season in Northern China: A review, Renewable and

1148 Sustainable Energy Reviews, 149, 111339, https://doi.org/10.1016/j.rser.2021.111339,

1149 2021b.

1150 Zhao, D. and Sun, B.: Atmospheric Pollution from Coal Combustion in China,

1151 Journal of the Air Pollution Control Association, 36, 371-374,

1152 10.1080/00022470.1986.10466074, 1986.

1153 Zheng, P., Chen, Y., Wang, Z., Liu, Y., Pu, W., Yu, C., Xia, M., Xu, Y., Guo, J.,

1154 Guo, Y., Tian, L., Qiao, X., Huang, D. D., Yan, C., Nie, W., Worsnop, D. R., Lee, S.,

1155 and Wang, T.: Molecular Characterization of Oxygenated Organic Molecules and

1156 Their Dominating Roles in Particle Growth in Hong Kong, Environ. Sci. Technol.,

1157 10.1021/acs.est.2c09252, 2023.

1158